The Astrophysical Journal Supplement Series, 180:38–53, 2009 January doi:10.1088/0067-0049/180/1/38

ANALYSIS OF ELECTRON-IMPACT EXCITATION AND EMISSION OF THE $np\sigma\ ^1\Sigma_u^+$ AND $np\pi\ ^1\Pi_u$ RYDBERG SERIES OF H_2

Michèle Glass-Maujean[1], Xianming Liu[2], and Donald E. Shemansky[2]
[1] Laboratoire de Physique Moléculaire pour l'Atmosphère et l'Astrophysique, Université Pierre et Marie Curie/CNRS, 4 Place Jussieu, F-75252 Paris Cedex 05, France; michele.glass@upmc.fr
[2] Planetary and Space Science Division, Space Environment Technologies, Pasadena, CA 91107, USA; xliu@spacenvironment.net, dshemansky@spacenvironment.net
Received 2008 April 14; accepted 2008 August 25; published 2008 December 23

ABSTRACT

Calculated and recently measured photoabsorption transition probabilities of the H_2 $np\sigma\ ^1\Sigma_u^+$ and $np\pi\ ^1\Pi_u - X\ ^1\Sigma_g^+$ band systems have been examined with high-resolution ($\Delta\lambda = 95$–115 mÅ) electron-impact induced emission spectra obtained previously by Jonin et al. and Liu et al. When localized rovibronic coupling is insignificant, transition probabilities calculated with the adiabatic approximation are found to be generally consistent with experiment. However, in the presence of significant coupling, the transition probabilities obtained from a nonadiabatic calculation of $B'\ ^1\Sigma_u^+$, $D\ ^1\Pi_u^+$, $B''\bar{B}\ ^1\Sigma_u^+$, $D'\ ^1\Pi_u^+$, and $5p\sigma\ ^1\Sigma_u^+$ state coupling give better agreement with the experimental spectra. Emission yields obtained by comparison of the calculated and experimental spectra are also consistent with the measured predissociation and autoionization yields. In addition, more accurate excitation and emission cross sections and nonradiative yields have been obtained for a number of the $np\sigma\ ^1\Sigma_u^+$ and $np\pi\ ^1\Pi_u$ states. The results obtained in the present investigation lead to a significantly more accurate calibration of the *Cassini UVIS* instrument and laboratory spectrometers in the range 790–920 Å. They are also an important step toward an accurate model of extreme ultraviolet H_2 auroral and dayglow emissions in the outer planet atmospheres.

Key words: methods: laboratory – molecular process – ultraviolet: ISM

1. INTRODUCTION

Molecular hydrogen emission in the vacuum ultraviolet (VUV) arises in transitions from the $1s\sigma_g np\sigma_u\ ^1\Sigma_u^+$ and $1s\sigma_g np\pi_u\ ^1\Pi_u$ Rydberg series to the ground $X\ ^1\Sigma_g^+$ state. Although the Lyman- $\left(B\ ^1\Sigma_u^+ - X\ ^1\Sigma_g^+\right)$ and Werner- $\left(C\ ^1\Pi_u - X\ ^1\Sigma_g^+\right)$ band systems dominate in the far ultraviolet (FUV) region, the contribution from the higher $np\sigma_u$ and $np\pi_u$ ($n \geqslant 3$) Rydberg states becomes important in the extreme ultraviolet (EUV) region. The large number of states contributing to emission in the EUV region produces a much more congested and complicated spectrum than is found in the FUV region. Additional decay mechanisms for some excited levels also complicate the EUV emission spectrum. In the absence of collisions, predissociation competes with spontaneous emission to depopulate the levels that lie above the H($1s$)+H(2ℓ) dissociation limit (Julienne 1971; Glass-Maujean et al. 1987). Above the first ionization limit, autoionization becomes another mechanism of depopulating the $np\sigma_u$ and $np\pi_u$ states (Herzberg & Jungen 1972; Dehmer & Chupka 1976). Both predissociation and autoionization of H_2 singlet-*ungerade* states have been investigated extensively (Dehmer & Chupka 1976; Glass-Maujean et al. 1978; Glass-Maujean 1979; Glass-Maujean 1986; Glass-Maujean et al. 1987, 2007a, 2007b, 2007c, 2008a, 2008b; Guyon et al. 1979; Dehmer & Chupka 1995; Dehmer et al. 1989, 1992; Pratt et al. 1990, 1992, 1994; Stephens & Greene 1994).

Electron-impact excitation of molecular hydrogen is an important process in molecular clouds and outer planet atmospheres. Several observations of Jupiter aurorae with the *Hubble Space Telescope* (*HST*) in the FUV region have confirmed the importance of the electron-impact excitation process (Clarke et al. 1994; Trafton et al. 1994; Kim et al. 1995). In addition, the Hopkins Ultraviolet Telescope (HUT) observations of Jupiter aurorae and dayglow in both the FUV and EUV regions have revealed the electron-impact excitation of H_2 to various singlet-*ungerade* states (Feldman et al. 1993; Morrissey et al. 1997; Wolven & Feldman 1998). Analyses of *Galileo* and *Far Ultraviolet Spectroscopic Explorer* (*FUSE*) observations of Jupiter auroral emissions in both the EUV and FUV regions by Ajello et al. (1998) and Gustin et al. (2004) have shown intense H_2 emission over a range of molecular hydrogen column densities of 10^{16}–10^{21} cm^2. All observations in the EUV wavelength region show significant emission from high Rydberg ($n \geqslant 3$) states between 760 Å and 900 Å. However, the lack of reliable excitation and emission cross sections, particularly for the large number of transitions on the blue side of 900 Å, results in difficulty in modeling both experimental and spacecraft observations (Liu et al. 2000). Accurate excitation and emission cross sections of the high Rydberg states, therefore, are important to the interpretation of the outer planet observations in the EUV region.

While many investigations on electron-impact induced emission of H_2 have been carried out, reliable excitation and emission cross sections for the $n > 3$ Rydberg states are generally not available. Early low-resolution investigations of the electron-impact induced emission spectrum of H_2 have been reported by Ajello et al. (1982, 1984, 1988), who also performed crude and inadequate modeling of the emission spectrum with band transition probabilities by Allison & Dalgarno (1970). Liu et al. (1995) and Abgrall et al. (1997, 1999) have shown that the band transition probabilities partitioned by Hönl–London factors are inaccurate. Transition probabilities calculated by Abgrall et al. (1993a, 1993b, 1993c, 1999) accurately reproduce the experimental intensity distribution. Jonin et al. (2000) and Liu et al. (2000) have extended the high-resolution experimental investigations and theoretical modeling into the EUV region. Their investigation found that $B\ ^1\Sigma_u^+ - X\ ^1\Sigma_g^+$, $C\ ^1\Pi_u - X\ ^1\Sigma_g^+$, $B'\ ^1\Sigma_u^+ - X\ ^1\Sigma_g^+$ and $D\ ^1\Pi_u - X\ ^1\Sigma_g^+$ transition probabilities of Abgrall et al. (1993a, 1993b, 1993c, 1994) can reproduce the

observed relative intensities in wavelength regions where the contribution from $n > 3$ Rydberg states is negligible. The calculated spectra of Jonin et al. (2000) reproduced 95%–96% of observed H_2 emission intensities in the 900−1040 Å region. The remaining 4%–5% intensity differences are attributed to emission from higher ($n > 3$) Rydberg states, perturbations between the $n \leqslant 3$ (primarily the $B'\ ^1\Sigma_u^+$) states and $n > 3$ states, and cascade excitation of the low v_j level of the $B'\ ^1\Sigma_u^+$ state via the singlet-*gerade* states (Liu et al. 2002). Jonin et al. (2000) also obtained experimental estimates of the emission cross sections of the $B'\ ^1\Sigma_u^+$, $D\ ^1\Pi_u$, $B''\bar{B}\ ^1\Sigma_u^+$, $D'\ ^1\Pi_u$, and $D''\ ^1\Pi_u$ states. They, however, encountered a number of difficulties, especially for the transitions below 900 Å. Experimentally, significant contributions from the high-Rydberg ($n \geqslant 3$) states make the EUV emission spectrum much more congested. In the absence of reliable theoretical calculations, it is difficult to appropriately partition the overlapping experimental intensity to individual transitions. The general weakness of transitions for these high-Rydberg states and optical thickness of certain resonance transitions also seriously compromise the analytical interpretation. The lack of transition probabilities and oscillator strengths makes it difficult to estimate the self-absorption of resonance transitions. Finally, the emission yields of many states are not accurately known because of dissociation, predissociation, and autoionization. The combined effects lead to very significant errors in estimated cross sections.

We have re-analyzed the high-resolution electron-impact induced emission spectra of Liu et al. (2000) and Jonin et al. (2000) with recently measured and calculated transition probabilities of the $np\sigma_u\ ^1\Sigma_u^+$ and $np\pi_u\ ^1\Pi_u - X\ ^1\Sigma_g^+$ ($n > 3$) band systems. Some calculated transition probabilities have been reported recently by Glass-Maujean et al. (2007a, 2007b, 2007c, 2008a), along with high-resolution photoabsorption measurements. The present analysis provides further examination of the accuracy of the calculated transition probabilities. Emission yields of various rovibrational levels of the $np\sigma_u\ ^1\Sigma_u^+$ and $np\pi_u\ ^1\Pi_u$ states are determined by comparing observed and calculated spectra. The derived emission yields are then compared with the autoionization yields determined by Dehmer & Chupka (1976) and the predissociation yields by Glass-Maujean et al. (1987). Excitation and emission cross sections of these band systems are obtained from the calculated transition probabilities and measured emission yields.

The singlet-*ungerade* states of the H_2 have been studied by various experimental techniques including photo absorption (Herzberg & Howe 1959; Namioka 1964a, 1964b; Takezawa 1970; Herzberg & Jungen 1972; Dabrowski 1984; Glass-Maujean et al. 1984, 1985a, 1985b, 1987, 2007a, 2007b, 2007c, 2008a), photoemission (Roncin et al. 1984; Larzillière et al. 1985; Abgrall et al. 1993a, 1993b, 1993c, 1994; Roncin & Launay 1994), photoionization (Dehmer & Chupka 1976, 1995), and nonlinear laser spectroscopy (Hinnen et al. 1994a, 1994b, 1995a, 1995b, 1996; Hogervorst et al. 1998; Reinhold et al. 1996, 1997; De Lange et al. 2001; Koelemeij et al. 2003; Greetham et al. 2003; Ubachs & Reinhold 2004; Hollenstein et al. 2006; Ekey et al. 2006). The spectral atlas of Roncin & Launay (1994), in particular, has provided an extensive tabulation of transition frequencies.

Molecular hydrogen has also been extensitively theoretically investigated. Multichannel quantum defect theory (MQDT) was first developed to interpret high-resolution H_2 photoabsorption spectra (Herzberg & Jungen 1972) and H_2 autoionization (Jungen & Atabek 1977; Ross & Jungen 1987, 1994a, 1994b, 1994c, 1997). Since the pioneer work of Kolos & Wolniewicz (1968), ab initio calculations of the potential energies have been developed for several decades. Accurate calculations, including the adiabatic and the diagonal nonadiabatic corrections (Wolniewicz 1993; Staszewska & Wolniewicz 2002; Wolniewicz & Staszewska 2003a), have been carried out. The calculations of H_2 transition moment functions (Wolniewicz & Staszewska 2003a, 2003b) and nonadiabatic coupling of the first several members of the singlet-*ungerade* Rydberg series have been recently reported (Wolniewicz et al. 2006).

2. EXPERIMENT

The experimental data used in the present analysis were obtained almost nine years ago. A subset of the measured spectra has been reported by Jonin et al. (2000) and Liu et al. (2000). Since the experimental setup was substantially similar to that described by Jonin et al. (2000) and Liu et al. (1995), only a brief overview will be given here.

The experimental system consists of a 3 m spectrometer (Acton VM-523-SG) and an electron collision chamber. Electrons generated by heating a thoriated tungsten filament are magnetically collimated with an axially symmetric magnetic field of ∼100 G and accelerated to a kinetic energy of 100 eV. The accelerated electrons, which move horizontally, collide with a vertical beam of H_2 gas formed by a capillary array. The cylindrical interaction region is about 3 mm in length and ∼2 mm in diameter. Optical emission from electron-impact excited H_2 is dispersed by the spectrometer equipped with a 1200 grooves mm^{-1} grating coated with B_4C. The spectrometer has an aperture ratio of $f/28.8$ and a field of view of 3.8 mm (horizontal) by 2.4 mm (vertical). The dispersed radiation is detected with a channel electron multiplier (Galileo 4503) coated with CsI. A Faraday cup was utilized to minimize the backscattered electrons and monitor the beam current.

Three sets of spectra at different resolutions were used in the present analysis. The first set, acquired in the first order with a slit width of 40 μm, an increment of 0.040 Å, and an integration time of 70 s per channel, had a FWHM of ∼0.115 Å. As reported in Jonin et al. (2000), its effective foreground H_2 column density was $(2.3 \pm 0.6) \times 10^{13}$ cm^{-2} and the spectral range was from 800 Å to 1440 Å. The second set, obtained with a 25 μm slit width, 0.020 Å wavelength increment, and 90 s integration time, had a FWHM of ∼0.095 Å. The H_2 foreground column density was estimated to be $\left(15 \pm \frac{5}{4}\right) \times 10^{13}$ cm^{-2} by a cross comparison of the intensities of strong nonresonance transitions between cross-beam and swarm measurements (Jonin et al. 2000). While its spectral range was from 788 Å to 1100 Å, only the features in the 790–910 Å region are used for the analysis, as the optical thickness was too high for many Lyman- and Werner-band resonance transitions. The third set of data, obtained with a slit width of 80 μm and ∼ 20% higher pressure (18×10^{13} cm^{-2}), has a resolution of ∼0.24 Å, and was used to examine the weak H_2 emissions between 750 Å and 800 Å.

The wavelength scale of the observed spectrum was established by assuming a uniform grating step size and by using the absolute wavelength of the H Lyman series emissions. The mechanical limitation of the stepping motor, and, more importantly, the slight temperature fluctuation of the spectrometer ($\pm 0.3^\circ$C) during the scan resulted in significant slowly varying nonuniform wavelength shifts. The wavelength error was estimated by comparing the observed spectra with the model spectra, utilizing the experimentally derived energy-term values. The

largest wavelength error, from the extremes of negative and positive shifts, was found to be ~0.04 Å. As frequencies of many strong transitions of H_2 have been accurately measured in previous studies, the effect of the small-wavelength deviation can be reduced by aligning the observed and model spectra over strong features. Hence, the wavelength shifts did not cause significant problems for the analysis reported in the present paper.

3. THEORY

3.1. Photon Emission Intensity of Electron-Impact Excitation

Steady-state photon emission intensity resulting from direct excitation by a continuous electron beam has been described in detail by Jonin et al. (2000). A brief review will be given here. The volumetric photon emission rate (I) from electron-impact excitation is proportional to the excitation rate and emission-branching ratio:

$$I(v_j, v_i; J_j, J_i) = g(v_j; J_j)\frac{A(v_j, v_i; J_j, J_i)}{A(v_j; J_j)}(1 - \eta(v_j, J_j)) \times (1 - \kappa(\epsilon_{ij}, \zeta_i)) \quad (1)$$

where the indexes j and i refer to the upper and lower electronic-state vibrational and rotational levels, respectively, and summation over the missing index is assumed. J and v refer to rotational and vibrational quantum numbers, respectively. $A(v_j, v_i; J_j, J_i)$ is the Einstein spontaneous transition probability for emission from level (v_j, J_j) to level (v_i, J_i), and $A(v_j, J_j)$ is the total radiative transition probability for level (v_j, J_j) (including transition to lower singlet-*gerade* states and to the continuum levels of the $X\,^1\Sigma_g^+$ state). The yield of nonradiative processes is represented by $\eta(v_j, J_j)$. Under the present experimental conditions, collision deactivation is 10^4–10^5 times slower than radiative decay, and is, therefore, negligible. The sum of appropriate predissociation, dissociation, and autoionization yields is denoted by $\eta(v_j, J_j)$. Since the experimental condition for certain strong resonance transitions to the $X\,^1\Sigma_g^+(0)$ levels is optically thick, the parameter $\kappa(\epsilon_{ij}, \zeta_i)$ in Equation (1) accounts for the self-absorption for those resonance transitions. The calculation of $\kappa(\epsilon_{ij}, \zeta_i)$ from H_2 foreground column density and transition probability has been given by Jonin et al. (2000).

The excitation rate, $g(v_j, J_j)$, represents the sum of the excitation rates from the rotational and vibrational levels of the $X\,^1\Sigma_g^+$ state. It is proportional to the population of the molecules in the initial level, $N(v_i, J_i)$, the excitation cross section (σ_{ij}), and the electron flux (F_e):

$$g(v_j; J_j) = F_e \sum_i N(v_i, J_i)\sigma(v_i, v_j; J_i, J_j). \quad (2)$$

The excitation cross section σ_{ij} is calculated from the analytical function (Liu et al. 1998)

$$\frac{\sigma(v_i, v_j; J_i, J_j)}{\pi a_0^2} = 4 f(v_i, v_j; J_i, J_j)\frac{Ry}{E_{ij}}\frac{Ry}{E}\left[\frac{C_0}{C_7}\left(\frac{1}{X^2} - \frac{1}{X^3}\right) + \sum_{k=1}^{4}\frac{C_k}{C_7}(X-1)\exp(-kC_8X) + \frac{C_5}{C_7}\left(1 - \frac{1}{X}\right) + \ln(X)\right] \quad (3)$$

where a_0 and Ry are the Bohr radius and Rydberg constant, respectively, and f_{ij} is the optical absorption oscillator strength, given by Equation (16). E_{ij} is the threshold energy for the $(v_i, J_i) \rightarrow (v_j, J_j)$ excitation, E is the excitation energy, and $X = E/E_{ij}$. The coefficients C_k/C_7 ($k = 0$ to 6) and C_8 are determined by fitting the experimentally measured relative excitation function. For the present work, C_k/C_7 ($k = 0$ to 6) and C_8 determined by Liu et al. (1998) for the $B\,^1\Sigma_u^+ - X\,^1\Sigma_g^+$ and $C\,^1\Pi_u - X\,^1\Sigma_g^+$ band systems of H_2 are used for the direct excitation of the other $np\sigma\,^1\Sigma_u^+$ and $np\pi\,^1\Pi_u - X\,^1\Sigma_g^+$ band systems. The absolute value of the collision strength parameter, C_7, of Equation (3), is fixed to the absorption oscillator strength f_{ij} by the relation

$$C_7 = \frac{4\pi a_0^2(2J_i + 1)Ry}{E_{ij}} f(v_i, v_j; J_i, J_j). \quad (4)$$

In addition to the direct excitation, indirect excitation from the higher levels of singlet-*gerade* states is also possible. While the cascade from higher levels of the singlet-*gerade* states results in the indirect excitation of many rovibronic levels of the singlet-*ungerade* states, a recent time-resolved study of Liu et al. (2002) has shown that it preferentially contributes to the low v_j levels of the $B\,^1\Sigma_u^+$ and $B'\,^1\Sigma_u^+$ states, and the indirect excitation to the $B''\bar{B}\,^1\Sigma_u^+$, $D'\,^1\Pi_u$, or higher states is negligible.

The excitation cross section for a band system in the present study will be defined as the statistical average of the rovibrational cross section components:

$$\sigma_{ex} = \frac{1}{N_T}\sum_{i,j}\sigma(v_i, v_j; J_i, J_j)N_i \quad (5)$$

where N_T is the total H_2 population of the $X\,^1\Sigma_g^+$ state. The corresponding emission cross section is then given by

$$\sigma_{em} = \frac{1}{N_T}\sum_{i,j}\sigma(v_i, v_j; J_i, J_j)(1 - \eta_j)N_i. \quad (6)$$

Since transition probabilities of $np\sigma\,^1\Sigma_u^+$ and $np\pi\,^1\Pi_u$ states to the excited singlet-*gerade* (such as the $EF\,^1\Sigma_g^+$ and $GK\,^1\Sigma_g^+$) states are negligible when compared with those to the $X\,^1\Sigma_g^+$ state, the emission cross sections of the $np\sigma\,^1\Sigma_u^+$ and $np\pi\,^1\Pi_u - X\,^1\Sigma_g^+$ band systems can be considered identical to the emission cross sections of the $np\sigma\,^1\Sigma_u^+$ and $np\pi\,^1\Pi_u$ states, given by Equation (6).

The present model utilizes the $B\,^1\Sigma_u^+$, $C\,^1\Pi_u$, and $D\,^1\Pi_u^- - X\,^1\Sigma_g^+$ transition probabilities of Abgrall et al. (1994) and the presently calculated adiabatic $np\sigma\,^1\Sigma_u^+$ and $np\pi\,^1\Pi_u - X\,^1\Sigma_g^+$ transition probabilities of the higher Rydberg $n \geqslant 4$ states. Significant coupling exists among some of the v_j levels of the $B'\,^1\Sigma_u^+$, $B''\bar{B}\,^1\Sigma_u^+$, $5p\sigma\,^1\Sigma_u^+$, $D\,^1\Pi_u^+$, and $D'\,^1\Pi_u^+$ states. The calculated nonadiabatic transition probabilities are used for these levels. Wherever possible, the experimentally measured term values of Roncin & Launay (1994), Dabrowski (1984), and Takezawa (1970) are utilized to calculate the transition frequencies. To compare with the observed spectrum, the calculated spectrum is convoluted with a triangular instrument function with an appropriate FWHM.

3.2. Calculation of the $np\sigma\ ^1\Sigma_u^+$ and $np\pi\ ^1\Pi_u - X\ ^1\Sigma_g^+$ Transition Probabilities

3.2.1. Adiabatic Calculation of Higher $np\sigma\ ^1\Sigma_u+$ and $np\pi\ ^1\Pi_u - X\ ^1\Sigma_g^+$ Band Systems

The potential curves of the $B\ ^1\Sigma_u^+$, $B'\ ^1\Sigma_u^+$, $B''\bar{B}\ ^1\Sigma_u^+$, and $5p\sigma\ ^1\Sigma_u^+$ states (Staszewska & Wolniewicz 2002), the $C\ ^1\Pi_u$, $D\ ^1\Pi_u$, and $D'\ ^1\Pi_u$ states (Wolniewicz & Staszewska 2003b), and the $X\ ^1\Sigma_g^+$ state (Wolniewicz 1993), are known theoretically with adiabatic and nonadiabatic corrections. The dipole transition moment functions of the transitions to the $X\ ^1\Sigma_g^+$ state have been tabulated by Wolniewicz & Staszewska (2003a, 2003b). For higher members of the Rydberg series, the ab initio potential energy curves are unavailable. The quantum defect theory developed by Jungen & Atabek (1977) allows the determination of the Born–Oppenheimer potential energy with large adiabatic corrections through the classical formula

$$V(R) = V_{H_2^+}(R) - \frac{R_{H_2}}{(n-\delta)^2} \tag{7}$$

where δ is the quantum defect, and $V_{H_2^+}(R)$ is the potential energy curve of $H_2\ X^2\Sigma_g^+$, to which the Rydberg series converge.

When the calculated dipole transition moment function, $D_{n\Lambda}(R)$, is not available, it can be approximated from the known function of the $4p\Lambda - X$ transition, using the quantum defect δ_Λ:

$$D_{n\Lambda}(R) = D_{4\Lambda}(R)\left[\frac{(4-\delta_\Lambda)}{(n-\delta_\Lambda)}\right]^{3/2}. \tag{8}$$

Numerical integration using the Numerov method is employed to solve the Schrödinger equation to obtain eigenvalues and eigenfunctions. The spontaneous transition probability, $A(v_j, v_i; J_j, J_i)$, is given by (Hilborn 1982)

$$A(v_j, v_i; J_j, J_i) = \frac{2\omega_{ij}^3}{3\epsilon_0 hc^3}\left\langle \chi_{v_j J_j}(R)\,|D(R)|\,\chi_{v_i J_i}(R)\right\rangle^2 \times \frac{\mathcal{H}_{ji}(J_j, J_i)}{2J_j+1} \tag{9}$$

where $\omega_{ij}\left[=\left(E_{v_j,J_j} - E_{v_i,J_i}\right)/\hbar\right]$ is the angular frequency for the transition $j \rightarrow i$, $\chi(R)$ is the vibrational wavefunction with the rotational energy correction, and $\mathcal{H}_{ji}(J_j, J_i)$ is the Hönl–London factor as defined by Hansson & Watson (2005).

Equation (9) can be rewritten as

$$A(v_j, v_i; J_j, J_i) = 2.142\times 10^{10}\left(E_{v_j,J_j} - E_{v_i,J_i}\right)^3 \times \left\langle \chi_{v_j J_j}(R)\,|D(R)|\,\chi_{v_i J_i}(R)\right\rangle^2 \times \frac{\mathcal{H}_{ji}(J_j, J_i)}{2J_j+1} \tag{10}$$

where $A(v_j, v_i; J_j, J_i)$ is in s^{-1}, $\left(E_{v_j,J_j} - E_{v_i,J_i}\right)$ is in hartree, and the dipole transition moment function, $D(R)$ is in bohr.

3.2.2. Nonadiabatic Calculation of the $B'\ ^1\Sigma_u^+$, $B''\bar{B}\ ^1\Sigma_u^+$, $5p\sigma\ ^1\Sigma_u^+$, $D\ ^1\Pi_u^+$, and $D'\ ^1\Pi_u^+ - X\ ^1\Sigma_g^+$ Band Systems

The small mass of the H_2 often prevents a satisfactory reproduction of the experimental measurement using the Born–Oppenheimer approximation even if the adiabatic and diagonal nonadiabatic coupling corrections are applied. Coupling between the different electronic states must be included. While nonadiabatic coupling often appears as positional shifts of observed energy levels, the deviation of spectral intensities is even more apparent. Nonadiabatic coupling is of two types: rotational interaction mixing the $^1\Sigma_u^+$ and $^1\Pi_u^+$ states, and vibrational interaction mixing states with the same symmetry. Following the work and notation of Wolniewicz et al. (2006), the matrix elements between two coupling states for rotational mixing can be written:

$$\left\langle \Pi^+\left|D_{i,k}^{1,0}\right|\Sigma^+\right\rangle = \sqrt{2J(J+1)}\frac{\langle L^+\rangle}{R^2}. \tag{11}$$

Likewise, for vibrational coupling,

$$C_{i,k}^{\Lambda,\Lambda} = D_{i,k}^{\Lambda,\Lambda}(R) + G_{i,k}^{\Lambda,\Lambda}(R) + 2B_{i,k}^{\Lambda,\Lambda}(R)\frac{d}{dR}. \tag{12}$$

These matrix elements for the $B'\ ^1\Sigma_u^+$, $B''\bar{B}\ ^1\Sigma_u^+$, $D\ ^1\Pi_u$, and $D'\ ^1\Pi_u$ states have been tabulated as functions of the internuclear distance R by Wolniewicz et al. (2006).

In the present work, nonadiabatic coupling is assumed to be so weak that it can be treated as a perturbation. Consequently, the coupling matrix elements can be evaluated in an adiabatic vibrational basis set. The present adiabatic vibrational basis set, having 122 terms, includes the full vibrational progressions of the $B'\ ^1\Sigma_u^+$, $B''\bar{B}\ ^1\Sigma_u^+$, $5p\sigma\ ^1\Sigma_u^+$, $D\ ^1\Pi_u^+$, and $D'\ ^1\Pi_u^+$ states. Distinguishing between $^1\Sigma_u^+$ and $^1\Pi_u^+$ symmetry, the nonadiabatic eigenfunction, Φ_j, expressed in terms of the adiabatic vibrational basis, ϕ_k^Λ, is

$$\Phi_j = \sum_k \alpha_{jk}\phi_k^\Sigma + \sum_l \beta_{jl}\phi_l^\Pi. \tag{13}$$

The transition probability from the level j of the singlet-*ungerade* state to the level i of the $X\ ^1\Sigma_g^+$ state is then

$$A(v_j, v_i; J_j, J_i) = \frac{2\omega_{ij}^3}{3\epsilon_0 hc^3}\left\langle \sum_k \alpha_{jk}D_{ki}\sqrt{\frac{\mathcal{H}_{\Sigma\Sigma}(J_j, J_i)}{2J_j+1}} + \epsilon\sum_l \beta_{jl}D_{li}\sqrt{\frac{\mathcal{H}_{\Pi\Sigma}(J_j, J_i)}{2J_j+1}}\right\rangle^2 \tag{14}$$

where D_{ji} is the dipole matrix element of the transition from level j to the ground state i and is given by

$$D_{ji} = \left\langle \phi_j\,|D(R)|\,\chi_{v_i,J_i}(R)\right\rangle. \tag{15}$$

In Equation (14) ϵ is 1 for a P-branch transition and -1 for an R-branch transition (Vigué et al. 1983; Glass-Maujean & Beswick 1989).

The dipole moment functions of the $D\ ^1\Pi_u - X\ ^1\Sigma_g^+$, $B''\bar{B}\ ^1\Sigma_u^+ - X\ ^1\Sigma_g^+$, and $5p\sigma\ ^1\Sigma_u^+ - X\ ^1\Sigma_g^+$ band systems have been calculated and tabulated by Wolniewicz & Staszewska (2003a, 2003b).

The absorption line oscillator strength, $f(v_i, v_j; J_i, J_j)$, of Equations (3) and (4) is related to the line transition probability, $A(v_j, v_i; J_j, J_i)$, of Equations (9) and (14) by Abgrall & Roueff (2006)

$$f(v_i, v_j; J_i, J_j) = 1.4992\frac{2J_j+1}{2J_i+1}\frac{A(v_j, v_i; J_j, J_i)}{v^2(v_i, v_j; J_i, J_j)} \tag{16}$$

where $v(v_i, v_j; J_i, J_j)$ refers to the transition wavenumber in reciprocal centimeters.

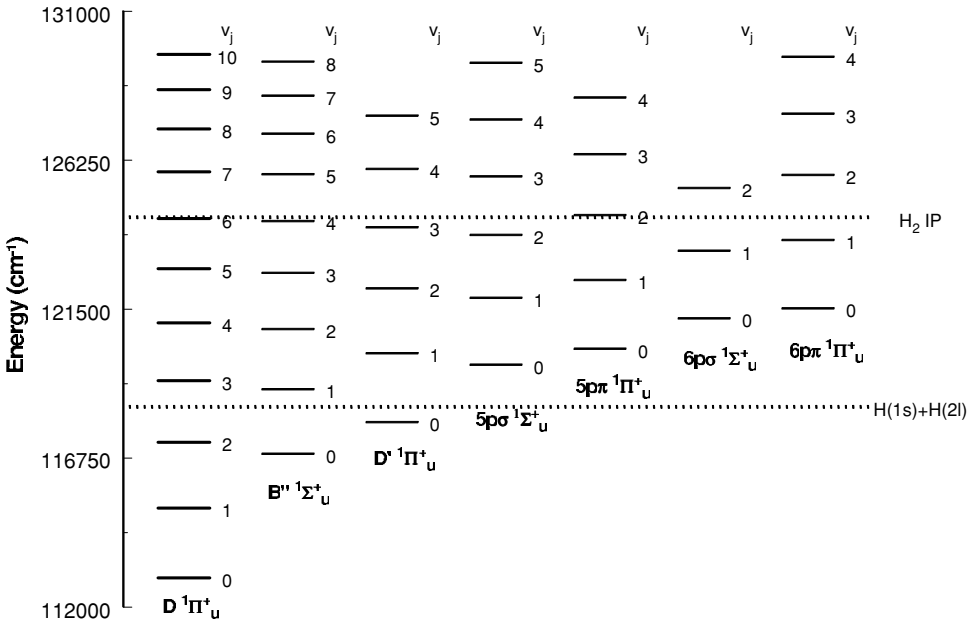

Figure 1. Experimental energy term values for $J_j = 0$ of the $np\sigma\ ^1\Sigma_u^+(v_j)$ state and $J_j = 1$ of the $np\pi\,^1\Pi_u^+(v_j)$ state. Note that the inner-well vibrational quantum number is used for the $B''\bar{B}\ ^1\Sigma_u^+$ state. The positions of the H(1s)+H(2ℓ) continuum and H_2 first ionization potential ($J_j = 0$) are indicated by the dotted lines. The H(1s)+H(3ℓ) and H(1s)+H(4ℓ) continua, at 133610.35 and 138941.96 cm^{-1}, respectively, are beyond the scale of the figure. All energy values are relative to the $J_i = 0$ and $v_j = 0$ level of the $X\ ^1\Sigma_g^+$ state.

4. ANALYSIS

4.1. Predissociation and Autoionization

In addition to spontaneous emission, nonradiative processes such as predissociation and autoionization occur for some levels. Figure 1 shows the experimental energy term values of the lowest J_j levels of some $np\sigma\ ^1\Sigma_u^+(v_j)$ and $np\pi\ ^1\Pi_u^+(v_j)$ states, along with the positions of the H(1s)+H(2ℓ) dissociation limit and the first H_2 ionization potential. In general, any $np\sigma\ ^1\Sigma_u^+$ or $np\pi\ ^1\Pi_u^+$ levels above the dissociation limit can be predissociative. Any $np\sigma\ ^1\Sigma_u^+$ or $np\pi\ ^1\Pi_u$ levels above the ionization potential can autoionize.

The extensive experimental and theoretical work of Glass-Maujean (1986) and coworkers (Glass-Maujean et al. 1978, 1979, 1984, 1985a, 1987) have shown that the predissociation of the $np\sigma_u\,^1\Sigma_u^+$ ($n > 3$) and $np\pi_u\ ^1\Pi_u$ ($n \geqslant 3$) states primarily takes place via coupling to the continuum levels of the $B'\,^1\Sigma_u^+$ state. The rate of predissociation differs drastically depending on the orbit symmetries and relative energy separations. For instance, the $D\,^1\Pi_u^+$ and $B'\,^1\Sigma_u^+$ states are strongly coupled by Coriolis interaction. Thus, the $D\,^1\Pi_u^+$ rovibrational levels that lie above the H(1s)+H(2ℓ) limit are predissociated very rapidly. The lifetimes of the $J_j = 2$ of the $v_j = 3 - 11$ levels of the $D\,^1\Pi_u^+$ state were determined to be $(3.7-5.9) \times 10^{-13}$ s (Glass-Maujean et al. 1979, 1985b), which are 10,000 times shorter than their expected fluorescence lifetime, $(2-4) \times 10^{-9}$ s (Glass-Maujean et al. 1985c; Abgrall et al. 1994). In contrast, the $D\,^1\Pi_u^-$ state and other higher $np\pi\,^1\Pi_u^-$ states are not coupled to the $B'\,^1\Sigma_u^+$ or other $np\sigma\ ^1\Sigma_u^+$ states. These states can only couple to a dissociating $^1\Pi_u^-$ state. For the $np\pi\,^1\Pi_u^-$ states below the H(1s)+H($n = 3$) limit, $C\,^1\Pi_u^-$ is the only dissociative $^1\Pi_u^-$ state. Since $np\pi_u\,^1\Pi_u^-$ states are only weakly coupled to the $C\,^1\Pi_u^-$ state, their predissociation rates are negligibly small. Above the H(1s)+H($n = 3$) limit, $np\pi\ ^1\Pi_u^-$ levels can also be dissociated by the $D\,^1\Pi_u^-$ continuum. Glass-Maujean et al. (2007c) recently found that the coupling between the $D'\,^1\Pi_u^-$ state and $D\,^1\Pi_u^-$ continuum is fairly efficient. Moreover, the predissociation of the $B''\bar{B}\ ^1\Sigma_u^+$ and $np\sigma\ ^1\Sigma_u^+$ ($n > 4$) states, in general, takes place by homogeneous coupling with the $B'\,^1\Sigma_u^+$ continuum levels (Glass-Maujean et al. 1978). Due to the difference in the $np\sigma\ ^1\Sigma_u^+ - B'\,^1\Sigma_u^+$ continuum Franck–Condon overlap integrals, variations in the predissociation rates are expected. The predissociation of the $np\pi\ ^1\Pi_u^+$ ($n > 3$) arises from either $np\pi\,^1\Pi_u^+ - D\,^1\Pi_u^+$ homogeneous coupling followed by $D\,^1\Pi_u^+ - B'\,^1\Sigma_u^+$ Coriolis coupling or $np\pi\,^1\Pi_u^+ - np\sigma\ ^1\Sigma_u^+$ Coriolis coupling followed by $np\sigma\ ^1\Sigma_u^+ - B'\,^1\Sigma_u^+$ homogeneous coupling (Glass-Maujean 1979). Levels below the H(1s)+H(2ℓ) limit cannot be predissociated. In particular, the $v_j = 0$ levels of the $B''\bar{B}\ ^1\Sigma_u^+$ and $D'\,^1\Pi_u$ states lie below the limit, and spontaneous emission is the only decay mechanism.

The ionization energy of the $v_i = 0$ and $J_i = 0$ level of the $X\ ^1\Sigma_g^+$ state of H_2 is 124,417.507 cm^{-1}. For the low J_j levels of the of $B''\bar{B}\ ^1\Sigma_u^+$ and $D'\,^1\Pi_u$ states, autoionization is energetically not possible unless v_j is $\geqslant 4$ for the $B''\bar{B}\ ^1\Sigma_u^+$ state and $v_j \geqslant 3$ for the $D'\,^1\Pi_u$ state (see Figure 1). Furthermore, vibrational autoionization of H_2 has a tendency to proceed with a small change in vibrational quantum number (i.e., $\Delta v = v_+ - v_j$) and the autoionization rate rapidly decreases for processes with large Δv changes (Dehmer & Chupka 1976; O'Halloran et al. 1988, 1989). Autoionization of the $B''\bar{B}\ ^1\Sigma_u^+$ state requires a fairly large change in Δv and its efficiency is low ($\leqslant 5\%$; Dehmer & Chupka 1976). Autoionization rates for the $v_j > 4$ levels of the $D'\,^1\Pi_u$ state is significant and the efficiency for the low J_j levels of these bands has been measured by Dehmer & Chupka (1976).

4.2. Spectral Analysis

The examination of the relative accuracy of the calculated transition probabilities rests on the relationship of the photoemission intensity to the emission-branching ratio via Equation (1) and the oscillator strength via Equation (3). The

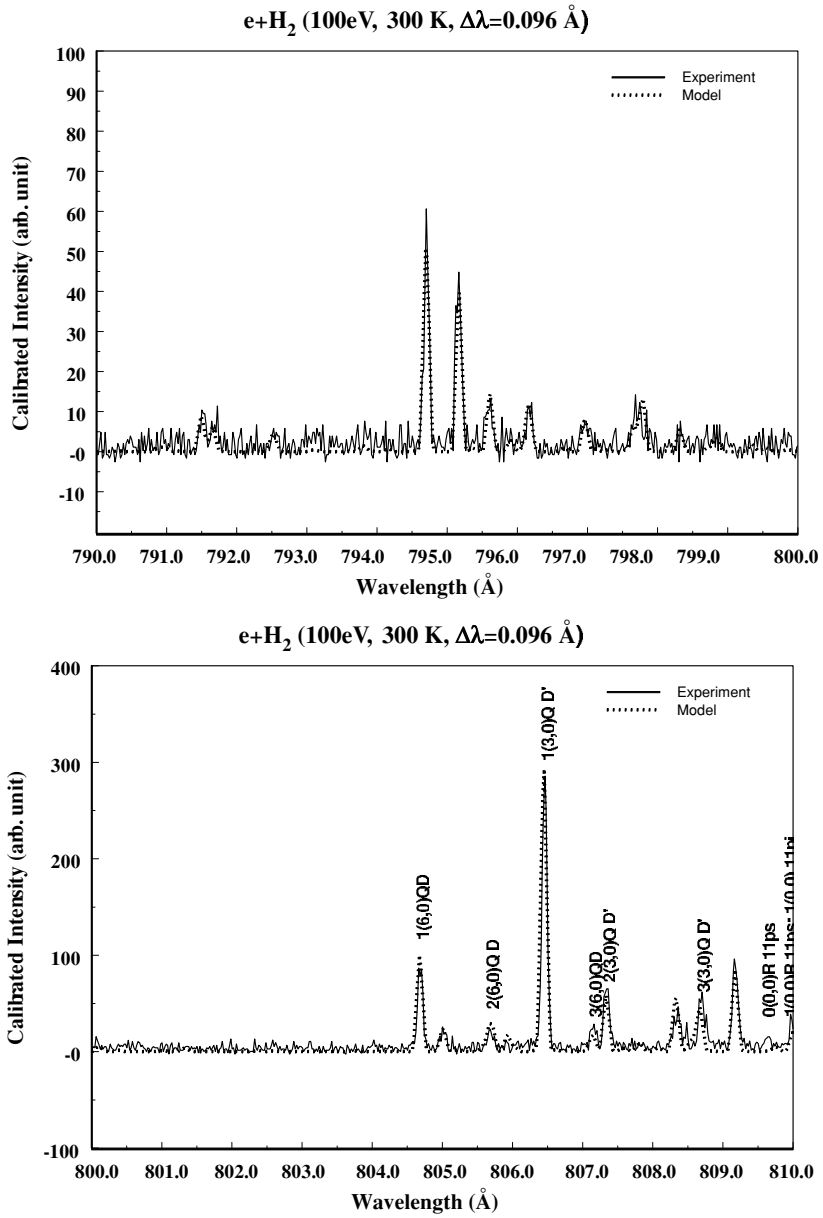

Figure 2. Comparison of experimental (solid trace) and model (dot trace) spectra in the range 790 Å to 850 Å. The model uses transition probabilities of the $B\ ^1\Sigma_u^+$, $C\ ^1\Pi_u$, and $D\ ^1\Pi_u^- - X\ ^1\Sigma_g^+$ band systems calculated by Abgrall et al. (1993a, 1993b, 1993c, 1994), nonadiabatic transition probabilities of the $B'\ ^1\Sigma_u^+$, $D\ ^1\Pi_u^+$, $B''\bar{B}\ ^1\Sigma_u^+$, $5p\sigma\ ^1\Sigma_u^+$, and $D'\ ^1\Pi_u^+ - X\ ^1\Sigma_g^+$ band systems, and adiabatic transition probabilities of the $6p\sigma\ ^1\Sigma_u^+$, $7p\sigma\ ^1\Sigma_u^+$, $D'\ ^1\Pi_u^-$, $D''\ ^1\Pi_u$, $7p\pi\ ^1\Pi_u$, and $8p\pi\ ^1\Pi_u - X\ ^1\Sigma_g^+$ band systems calculated in the present work. Spectral assignments of some transtions are indicated.

first set of spectra with an H_2 foreground column density of $(2.3 \pm 0.6) \times 10^{13}$ cm^{-2} is optically thin for all except a few strong Werner-band resonance transitions. In principle, it gives accurate relative intensities. In practice, spectral intensities and signal-to-noise ratios for most transitions on the blue side of 850 Å are too weak for reliable relative intensity measurement. In the present analysis, examination of the relative accuracy of the transition probabilities and derivation of nonradiative yields of the $np\sigma\ ^1\Sigma_u^+$ ($n > 3$) and $np\pi\ ^1\Pi_u$ ($n > 3$) states are primarily carried out in the 790−900 Å region of the second set of spectra, although transitions in 900−1180 Å region of the first set are also utilized to confirm the derived nonradiative yields. The second set of spectra has a foreground column density of $\sim 15 \times 10^{13}$ cm^{-2}. The largest self-absorption in the 790−900 Å region is ∼28%, for the $Q(1)$ and $R(1)$ transitions of the $D\ ^1\Pi_u(2) - X\ ^1\Sigma_g^+(0)$ band. Comparison of relative intensities between the first and second sets of spectra in the (2, 0) and (1, 0) band regions of the $D\ ^1\Pi_u - X\ ^1\Sigma_g^+$ band system verified that the self-absorption model described in Jonin et al. (2000) reliably accounts for the intensity.

Analysis was initiated by adding the $D'\ ^1\Pi_u^- - X\ ^1\Sigma_g^+$ transition to an existing model of the $B\ ^1\Sigma_u^+ - X\ ^1\Sigma_g^+$, $C\ ^1\Pi_u - X\ ^1\Sigma_g^+$, $B'\ ^1\Sigma_u^+ - X\ ^1\Sigma_g^+$, and $D\ ^1\Pi_u - X\ ^1\Sigma_g^+$ band systems (Jonin et al. 2000). Since predissociation of the $D'\ ^1\Pi_u^-$ levels below the H($1s$)+H($n = 3$) dissociation limit is negligibly small, only autoionization was considered. Figure 1 shows that autoionization of $D'\ ^1\Pi_u^-$ is negligible for $v_j \leqslant 3$ vibrational levels. So, a comparison of the relative spectral intensity of calculated and observed $D'\ ^1\Pi_u^- - X\ ^1\Sigma_g^+$ transitions can be performed straightforwardly. It was found that the calculated spectrum can reproduce the relative intensities of observed $D'\ ^1\Pi_u^- - X\ ^1\Sigma_g^+$ transitions from

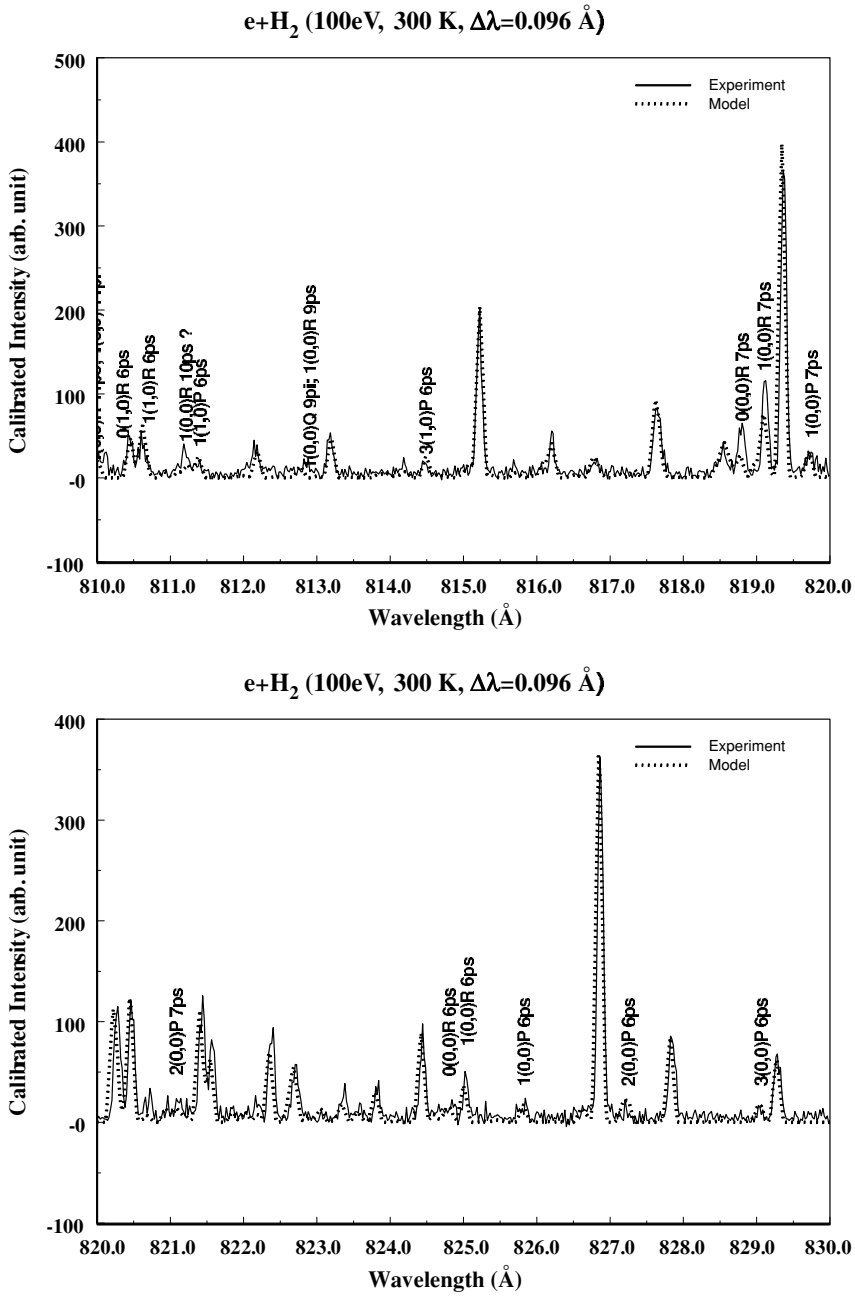

Figure 2. (Continued)

790 Å to 1100 Å if the emission yields of 0.62, 0.62, and 0.35 are applied to the $J_j = 1$, 2, and 3 levels of the $D'\,^1\Pi_u^-(4)$ state and the calculated adiabatic transition probabilities of the $Q(1)$ transitions are reduced by 48%, as suggested by the measurement of Glass-Maujean et al. (2007c). Since the autoionization yield of the $Q(1)$ transition is 8%–17% (Dehmer & Chupka 1976; M. Glass-Maujean et al. 2008, in preparation), the emission yield implies a dissociation yield of 0.2–0.3 for the $J_j = 1$ level of the $D'\,^1\Pi_u^-(4)$ state, which is consistent with an upper limit of 0.3 obtained by Glass-Maujean et al. (1987). In particular, emission in the 790−850 Å wavelength region is dominated by the Q-branch transitions of the $D\,^1\Pi_u$ and $D'\,^1\Pi_u$ states. The experimental spectrum provides a good test of consistency among the transition probabilities of the $D\,^1\Pi_u^- - X\,^1\Sigma_g^+$ and $D'\,^1\Pi_u^- - X\,^1\Sigma_g^+$ band systems. The good agreement in the relative intensities between the model and observed spectra shows that the calculated transition probabilities of the $D'\,^1\Pi_u^- - X\,^1\Sigma_g^+$ band system are consistent with those of $D\,^1\Pi_u^- - X\,^1\Sigma_g^+$.

Emission features on the blue side of 750−790 Å are generally very weak, and can only be practically measured with 80 μm slit widths (∼0.24 Å resolution). Most of the lines are from the Q-branch lines of the $D\,^1\Pi_u^- - X\,^1\Sigma_g^+$ and $D'\,^1\Pi_u^- - X\,^1\Sigma_g^+$ bands. The line at ∼784.04 Å, which arises from the $Q(1)$ transition of the $D'\,^1\Pi_u^-(5) - X\,^1\Sigma_g^+(0)$ band, is the strongest feature in the 750–790 Å region. As noted by Liu et al. (2000), the observed emission intensities of the $Q(2)$ and $Q(3)$ transitions are much weaker than those expected from a simple population difference of $J_i = 1$, 2, and 3 levels at room temperature. A recent combination of absorption, ionization, and dissociation measurements by M. Glass-Maujean et al. (2008, in preparation) have shown a sharp increase in ionization efficiency going from

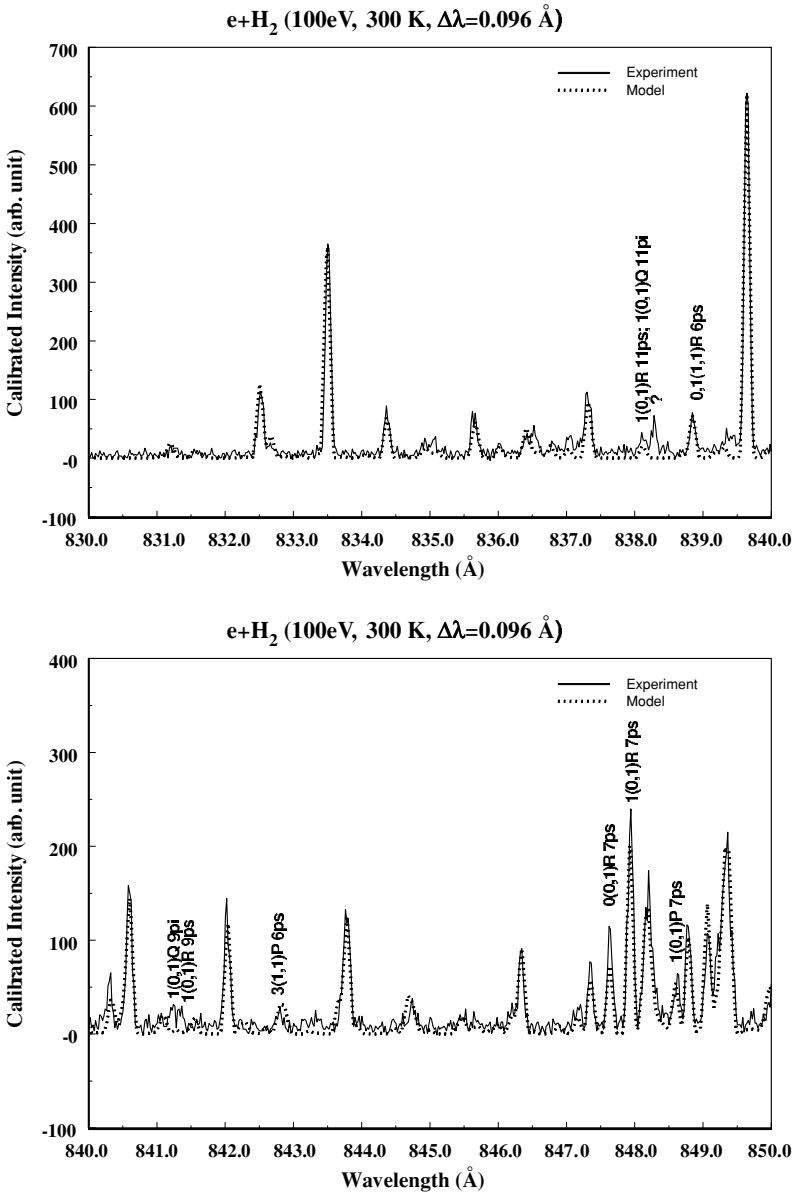

Figure 2. (Continued)

the $J_j = 1$ to the 2 and 3 levels. The $R(1)$ and $P(3)$ transitions of the $D'\ ^1\Pi_u^+(5)$ level, with a 7%–8% emission yield, are weak but observable.

The establishment of transition probabilities for the $D'\ ^1\Pi_u^- - X\ ^1\Sigma_g^+$ band allows the determination of variation of the overall relative sensitivity of the spectrometer. The inclusion of the $D'\ ^1\Pi_u^- - X\ ^1\Sigma_g^+$ emission in the model spectrum and utilization of a higher-resolution experimental spectrum (0.095 Å versus 0.115 Å) with significantly better signal-to-noise ratio produced a somewhat more accurate and flatter sensitivity curve in the 800–850 Å region than that reported by Jonin et al. (2000). After the improved sensitivity curve is applied to the observed spectrum, the Q-branch transitions of the $5p\pi\ ^1\Pi_u^-$, $6p\pi\ ^1\Pi_u^-$, $7p\pi\ ^1\Pi_u^-$, $8p\pi\ ^1\Pi_u^-$, and $10p\pi\ ^1\Pi_u^-$ states are introduced into the model. Glass-Maujean et al. (2007c) have shown that the measured transition-probability values of a number of Q-branch lines differ significantly from calculated values. Except for the $Q(1)$ transitions of $D\ ^1\Pi_u^-(6)$ and $D'\ ^1\Pi_u^-(3)$ levels, the transition probabilities of all other Q-branch lines used in the model have been adjusted to their experimental values. The P- and R-branch transitions of the $B''\bar{B}\ ^1\Sigma_u^+$, $5p\sigma\ ^1\Sigma_u^+$, $6p\sigma\ ^1\Sigma_u^+$, $7p\sigma\ ^1\Sigma_u^+$, and $np\pi\ ^1\Pi_u^+$ ($n = 4$–8) state are then added into the model. Because of the adiabatic nature of the calculation for many of these states, the transition probabilities of the P- and R-branches are essentially obtained from the calculated band transition probabilities partitioned by Hönl–London factors. Such an approximation is not expected to be valid in the presence of rovibronic coupling. For low v_j levels of the $B''\bar{B}\ ^1\Sigma_u^+$ and $D'\ ^1\Pi_u^+$ states and all discrete v_j level of the $B'\ ^1\Sigma_u^+$ and $D\ ^1\Pi_u^+$ states, the nonadiabatic calculation based on the ab initio results of Wolniewicz et al. (2006) described in Section 3.2.2 was used (see Section 5.1). The emission yields of some rovibrational levels of these states can be determined by comparing synthetic and calibrated experimental spectra.

5. RESULTS

Except for the few isolated regions noted below, model spectra in the region above 900 Å obtained using the Abgrall et al.

(1993a, 1993b, 1993c, 1994, 1997) $B\,^1\Sigma_u^+$, $C\,^1\Pi_u$, $B'\,^1\Sigma_u^+$, and $D\,^1\Pi_u - X\,^1\Sigma_g^+$ transition probabilities agrees with experimental observation (Jonin et al. 2000). In the "strong" emission regions of the $v_j = 0$ and 1 levels of the $B'\,^1\Sigma_u^+$ state, the calculated intensities, obtained by considering only direct excitation, are 20%−35% weaker than their experimental counterparts. As noted by Jonin et al. (2000), these regions include 976−982 Å of the (0, 2) band, 1012−1018 Å of the (0, 3) band, 1029−1035 Å of the (1, 4) band, and 1064−1070 Å of the (1, 5) band. The Liu et al. (2002) time-resolved measurements have shown that the preferential cascade excitation of the $v_j = 0$ and 1 levels of the $B'\,^1\Sigma_u^+$ state via higher singlet-*gerade* states is at least partially responsible for the enhancement in the experimental intensities. Good agreement between the calculated and measured intensities is obtained using 35% and 20% of direct excitation rates for the cascade excitation rates to the $v_j = 0$ and 1 levels. In comparision with the $n = 2$ and 3 states, transitions from $n \geqslant 4np\sigma\,^1\Sigma_u^+$ and $np\pi\,^1\Pi_u$ states in the 900−1050 Å region are generally weak but noticeable. The use of additional transition probabilities of the higher states, adiabatic or nonadiabatic, naturally leads to better agreement between model and experimental spectra than those shown in Figure 3 of Jonin et al. (2000).

Figure 2 compares the experimental and model spectra in the range 790–850 Å. The model utilizes the transition probabilities of the $B\,^1\Sigma_u^+$, $C\,^1\Pi_u$, and $D\,^1\Pi_u^- - X\,^1\Sigma_g^+$ band systems calculated by Abgrall et al. (1993a, 1993b, 1993c, 1994), nonadiabatic transition probabilities of the $B'\,^1\Sigma_u^+$, $D\,^1\Pi_u^+$, $B''\bar{B}\,^1\Sigma_u^+$, $5p\sigma\,^1\Sigma_u^+$, and $D'\,^1\Pi_u^+ - X\,^1\Sigma_g^+$ band systems, and adiabatic transition probabilities of the $6p\sigma\,^1\Sigma_u^+$, $7p\sigma\,^1\Sigma_u^+$, $D'\,^1\Pi_u^-$, $D''\,^1\Pi_u$, $7p\pi\,^1\Pi_u$, and $8p\pi\,^1\Pi_u - X\,^1\Sigma_g^+$ band systems obtained in the present work. Transitions involving higher Rydberg ($n \geqslant 9$) states are neglected in the model. Spectral assignments for some transitions, including those neglected by the model, are indicated. Question marks in the figure indicate that assignment has not been positively established.

5.1. Nonadiabatic Coupling of the $B'\,^1\Sigma_u^+$, $B''\bar{B}\,^1\Sigma_u^+$, $D\,^1\Pi_u^+$, and $D'\,^1\Pi_u^+$ States

Nonadiabatic coupling among $B'\,^1\Sigma_u^+(4)$, $B''\bar{B}\,^1\Sigma_u^+(0)$, $D\,^1\Pi_u^+(2)$, and $D'\,^1\Pi_u^+(0)$ levels results in significant differences in the calculated spectrum. Figure 3 compares the relative intensities of experimental and calculated spectra in the region of $B'\,^1\Sigma_u^+(4)$, $B''\bar{B}\,^1\Sigma_u^+(0)$, and $D\,^1\Pi_u(2) - X\,^1\Sigma_g^+(0)$ transitions. Although experimental spectrum (solid trace) has been calibrated using the procedures described by Liu et al. (1995) and Jonin et al. (2000), the variation of instrumental sensitivity, which is less than 1.7% over the region shown, is completely negligible. The model spectrum (dot trace, Model 1) in the top panel of Figure 3 was calculated from the $B\,^1\Sigma_u^+$, $C\,^1\Pi_u$, $B'\,^1\Sigma_u^+$, and $D\,^1\Pi_u - X\,^1\Sigma_g^+$ transition probabilities of Abgrall et al. (1994) and the present adiabatic transition probabilities of higher ($n \geqslant 4$) $np\sigma\,^1\Sigma_u^+$ and $np\pi\,^1\Pi_u$ series. Apart from the $B'\,^1\Sigma_u^+ - D\,^1\Pi_u^+$ coupling that was taken into account in the calculation of Abgrall et al. (1994), coupling among $B'\,^1\Sigma_u^+$, $B''\bar{B}\,^1\Sigma_u^+$, $D\,^1\Pi_u^+$, and $D'\,^1\Pi_u^+$ levels was not considered.

Transitions in Figure 3 are labeled in terms of $J_i(v_j, v_i)\Delta J\,\beta$, where i and j refer to the lower and upper states, β is the electronic designation of singlet-*ungerade* states, and $\Delta J = -1$, 0 and +1 correspond to P, Q, and R transitions, respectively. The ab initio calculation by Wolniewicz et al. (2006) indicates that the eigenvalues of the $J_j = 1$ levels of the $B'\,^1\Sigma_u^+(4)$ and $B''\bar{B}\,^1\Sigma_u^+(0)$ states in Abgrall et al. (1994) and Takezawa (1970) need to be interchanged. The model calculation and labeling shown in the figure conform to the indication. The alternative assignment would result in more significant difference at the $P(2)$ and $R(0)$ transitions. In any case, the top panel of Figure 3 shows that the adiabatic model generally underestimates the intensity of the $B''\bar{B}\,^1\Sigma_u^+(0)$ level. Moreover, the relative intensity between the $R(J_j - 1)$ and $P(J_j + 1)$ transitions also differs significantly from experiment. Similar discrepancy is apparent in the spectral regions involving transitions to the $v_i = 1$ and 2 levels of the $X\,^1\Sigma_g^+$ state. The calculated intensities for the $R(1)$ line of the $D'\,^1\Pi_u^+(0) - X\,^1\Sigma_g^+(1)$ band at 879.13 Å (not shown) is also too strong.

The bottom panel of Figure 3 compares the observed spectrum (solid trace) with model spectrum obtained from nonadiabatic coupling calculation (dot trace, Model 2). Specifically, the transition probabilities of the P and R branches of the $B'\,^1\Sigma_u^+$, $D\,^1\Pi_u^+$, $B''\bar{B}\,^1\Sigma_u^+$, $D'\,^1\Pi_u^+$, and $5p\sigma\,^1\Sigma_u^+$ states, used in the top panel, have been replaced by their counterparts obtained from nonadiabatic calculation. The use of nonadiabatic transition probabilities clearly results in better agreement between the calculated and observed spectra. Except for the $R(0)$ and $P(2)$ lines of the $B''\bar{B}\,^1\Sigma_u^+(0)$ and $B'\,^1\Sigma_u^+(4)$ levels, and the $R(1)$ and $P(3)$ lines from of the $D\,^1\Pi_u(2)$ level, all other discrepancies shown in the top panel have been removed. The disagreement between the nonadiabatic model and observation in the $R(1)$ and $P(3)$ lines of the $D\,^1\Pi_u(2) - X\,^1\Sigma_g^+(2)$ band, and the $R(0)$, $R(1)$, and $P(2)$ lines of the $B'\,^1\Sigma_u^+(4)$ and $B''\bar{B}\,^1\Sigma_u^+(0) - X\,^1\Sigma_g^+(1)$ bands, while reduced significantly, is still larger than the experimental error. The nonadiabatic transition probabilities also give rise to much better agreement for the $R(1)$ transition of the $D'\,^1\Pi_u(0) - X\,^1\Sigma_g^+(1)$ band.

5.2. Emission Yields

The top entries of the Tables 1 and 2 list predissociation yields for the $J_j = 0$–3 of $v_j = 1$–4 levels of the $B''\bar{B}\,^1\Sigma_u^+$ and $J_j = 1$–3 of $v_j = 1$–5 levels of the $D'\,^1\Pi_u^+$ states. In Table 1, v_j refers to the vibrational quantum number of the $B''\,^1\Sigma_u^+$ (inner well) state. The $v_j = 4$ level of the $B''\bar{B}\,^1\Sigma_u^+$ state lies above the first ionization potential of H_2. While autoionization is possible, the autoionization rate is apparently negligibly slow in comparison with predissociation (Dehmer & Chupka 1976). The $v_j = 0$ levels of both $B''\bar{B}\,^1\Sigma_u^+$ and $D'\,^1\Pi_u$ states are below the $B'\,^1\Sigma_u^+$ continuum; their emission yields are unity. The error in the predissociation yields in Tables 1 and 2 are estimated to be ∼8% (i.e., ±0.08). Within the experimental error, the emission yields of the $v_j = 1$, 2, and 3 levels of the $D'\,^1\Pi_u^-$ state are found to be near unity, consistent with the negligible predissociation yields determined by Glass-Maujean et al. (1987). Predissociation yields for other higher rovibrational levels of the $B''\bar{B}\,^1\Sigma_u^+$ and $D'\,^1\Pi_u^+$ state cannot be reliably determined in the present work. In the final analysis, the emission yields for these higher levels used in the synthetic spectrum were calculated from autoionization yields obtained by Dehmer & Chupka (1976) and predissociation yields reported by Glass-Maujean et al. (1987) or from the Glass-Maujean et al. (2007a, 2007b, 2007c, 2008a, 2008b) line-width measurements. The transition from the $D'\,^1\Pi_u$ and the inner well of the $B''\bar{B}\,^1\Sigma_u^+$ states to the lower excited singlet-*gerade* states and the continuum levels of the $X\,^1\Sigma_g^+$ are very weak. Predissociation yields for the levels listed

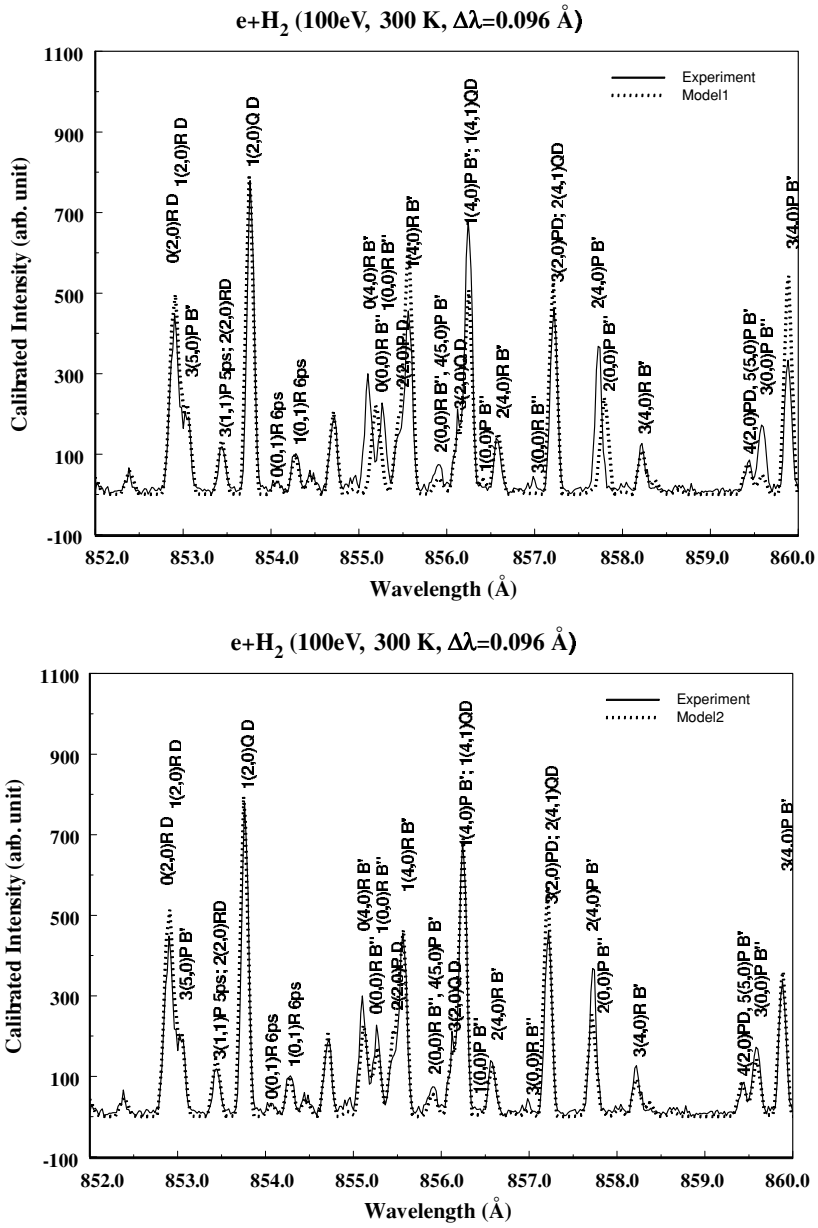

Figure 3. Comparison of observed (solid trace) and calculated (dot trace) spectra near the $D'\ ^1\Pi_u(2)$, $B'\ ^1\Sigma_u^+(4)$, and $B''\bar{B}\ ^1\Sigma_u^+(0) - X\ ^1\Sigma_g^+(0)$ band transition region. The calculated spectrum (Model 1) in the top panel was calculated with the $B'\ ^1\Sigma_u^+ - X\ ^1\Sigma_g^+$ and $D\ ^1\Pi_u - X\ ^1\Sigma_g^+$ transition probabilities of Abgrall et al. (1994) and adiabatic transition probabilities of the present work. Except for the partial $B'\ ^1\Sigma_u^+ - D\ ^1\Pi_u^+$ interaction, nonadiabatic coupling among the $B'\ ^1\Sigma_u^+$, $D\ ^1\Pi_u^+$, $B''\bar{B}\ ^1\Sigma_u^+$, $D'\ ^1\Pi_u^+$, and $5p\sigma\ ^1\Sigma_u^+$ states was neglected in the top panel. The dot trace in the bottom panel (Model 2) was obtained identically except for the use of the nonadiabatic transition probabilities for the $B'\ ^1\Sigma_u^+$, $D\ ^1\Pi_u^+$, $B''\bar{B}\ ^1\Sigma_u^+$, $5p\sigma\ ^1\Sigma_u^+$, and $D'\ ^1\Pi_u^+ - X\ ^1\Sigma_g^+$ transitions. Transitions are labeled as $J_i(v_j, v_i)\Delta J\beta$, where i and j refer to the lower and upper states, β is electronic designation of singlet-*ungerade* states, and $\Delta J = -1$, 0, and +1 correspond to P, Q, and R transitions, respectively.

in these tables are thus derived considering only the contribution of the discrete transition to the $X\ ^1\Sigma_g^+$ state to the total transition probability, $A(v_j, J_j)$, of Equation (1).

Nonradiative yields for other higher Rydberg states were obtained after the yields of the $B''\bar{B}\ ^1\Sigma_u^+$ and $D'\ ^1\Pi_u$ were established. Perturbations among the Rydberg series results in significant differences between the measured and calculated transition probabilities of many Q-branch excitations (Glass-Maujean et al. 2007c, 2008b). The calculated transition probabilities for the perturbed levels used in the model are adjusted to the measured values with the assumption that emission-branching ratios are insignificantly affected by the perturbation. Additionally, the transition probabilities of the P and R branches of the higher Rydberg states are generated from those of the Q branches with Hönl–London factors, even though perturbation will invariably introduce significant deviation. In absence of the nonadiabatic calculation, these two assumptions are necessary. The emission yields, obtained by assuming that the utilized transition probabilities are accurate, may thus deviate somewhat from the real values. Nevertheless, the fact that the most of the nonradiative yields in Tables 1 and 2 agree with the measured predissociation yields of Glass-Maujean et al. (1987) and the autoionization yields of Dehmer & Chupka (1976) indicates that the present approach is valid. More importantly, the use of the present emission yields and adjusted transition probabilities leads to the correct model intensities.

Predissociation yields of many rovibrational levels of the $B''\bar{B}\ ^1\Sigma_u^+$, $D'\ ^1\Pi_u$, and many other higher $np\sigma\ ^1\Sigma_u^+$ and $np\pi\ ^1\Pi_u$

Table 1
Nonradiative Yields of Some Rovibrational Levels of the $np\sigma\ ^1\Sigma_u^+$ States[a,b]

J_j		$v_j=0$	$v_j=1$	$v_j=2$	$v_j=3$	$v_j=4$
$B''\ ^1\Sigma_u^+$	0		0.90(>0.8)	>0.98 (>0.8)	0.93 (>0.8)	>0.95(>0.8)
	1		0.75(>0.5)	>0.97(>0.7)	0.95(>0.8)	>0.95(···)
	2		0.85(>0.6)	>0.95 (>0.7)	0.95 (···)	>0.93 (>0.9)
	3		0.80(>0.6)	>0.92 (···)	···(>0.7)	>0.95(···)
$5p\sigma\ ^1\Sigma_u^+$	0	0.5(0.65 ± 0.15)	0.15(···)	0.95(1.0 ± 0.1)[e]	>0.98(1.0 ± 0.1)[e]	
	1	0.35(0.50 ± 0.15)	0.3(0.3 ± 0.1)	>0.90(1.0 ± 0.1)[e]	>0.99(>0.6)	
	2	0.80(0.65 ± 0.15)	0.30[c](0.6 ± 0.1)	0.98(1.0 ± 0.1)[e]	>0.95(1.0 ± 0.1)[e]	
	3	0.55(>0.5)	0.3(0.5 ± 0.2)	>0.93(1.0 ± 0.1)[e]	>0.95(1.0 ± 0.1)[e]	
	4	···	···	0.9(1.0 ± 0.1)[e]	···	
$6p\sigma\ ^1\Sigma_u^+$	0	0[d]	0.55[d](0.5 ± 0.5)			
	1	0[d](<0.1)	0.50[d](0.55 ± 0.15)			
	2	0[d](<0.1)	0.55[d](0.55 ± 0.15)			
	3	0.15[d](0.2 ± 0.1)	0.60[d](0.6 ± 0.3)			
	4	0.20	0.65			

Notes.
[a] The estimated error limit for the present yield is 8% (i.e., ± 0.08). Note the v_j of the $B''\bar{B}\ ^1\Sigma_u^+$ state refers to the vibrational quantum number of the inner well ($B''\ ^1\Sigma_u^+$) state.
[b] Unless noted otherwise, values in parentheses refer to predissociation yields obtained by Glass-Maujean et al. (1987).
[c] See Section 5.2 for the cause of the large difference between the two sets of data.
[d] Obtained after the adjustments have been made on the calculated *P*- and *R*-branch transition probabilities to be consistent with observed relative emission intensities. These levels are perturbed, see Section 5.2. At the present time, the nonadiabatic perturbations of these levels cannot be calculated but they are estimated to be very strong.
[e] From Glass-Maujean et al. (2008a).

Table 2
Nonradiative Yields of Some Rovibrational Levels of the $np\pi\ ^1\Pi_u$ State[a,b]

J_j		$v_j=0$	$v_j=1$	$v_j=2$	$v_j=3$	$v_j=4$	$v_j=5$
$D'\ ^1\Pi_u^+$	1		0.88(0.65 ± 0.15)	0.78(0.6 ± 0.1)	0.92(0.82 ± 0.05)	>0.97(>0.82)	>0.95(0.93 ± 0.05)
	2		0.88(···)	0.93(0.85 ± 0.05)	0.95(0.88 ± 0.05)	>0.97(>0.89)	0.92(0.88 ± 0.10)
	3		0.80(0.9 ± 0.1)	0.95(0.95 ± 0.05)	0.90 (0.88 ± 0.08)	>0.9(>0.74 ± 0.1[d])	>0.95(>0.5 ± 0.2[d])
	4		>0.70	···	>0.87	>0.91	>0.96
$D'\ ^1\Pi_u^-$[c]	1					0.38(0.20[d])	0.14(0.14)
	2					0.38(0.26[d])	>0.87(0.93[d])
	3					>0.65(0.68[d])	>0.91(0.98[d])
$D''\ ^1\Pi_u^+$	1	0.15(<0.15)	0.4(0.4 ± 0.2)	>0.98(1.00)	>0.92(0.97)		
	2	0.2(<0.1)	0.8(0.7 ± 0.2)	>0.98(1.00 ± 0.05)	>0.95(0.95)		
	3	0.13	0.55	>0.98	>0.75		
$D''\ ^1\Pi_u^-$	1	0.05(<0.03)	0.06(<0.10 ± 0.05)	>0.98(⩽0.99)	0.85		
	2	0.15(<0.3)	0.0	>0.95	>0.4		
	3	···	···	>0.95	>0.85		
$6p\pi\ ^1\Pi_u^+$	1	0.7(0.5 ± 0.2)	0.3				
	2	0.6	0.3(0.4 ± 0.1)				
$6p\pi\ ^1\Pi_u^-$	1	0.05(<0.1)	0.24(0.3 ± 0.1)				
	2	0.10(<0.2)	⩽0.05(<0.15)				
$7p\pi\ ^1\Pi_u^+$	1	0.5	>0.98				
	2	0.7	>0.98				
$7p\pi\ ^1\Pi_u^-$	1	0.0	>0.98				
	2	···	>0.95				
	3	···	>0.95				

Notes.
[a] The estimated error in the yields is 8% (i.e., ± 0.08), except for the $v_j=4$ and 5 levels of the $D'\ ^1\Pi_u^+$ state, which is 12%.
[b] When autoionization is energetically impossible, values in parentheses represent the predissociation yields of Glass-Maujean et al. (1987). When autoionizatin is possible, they denote the sum of the predissociation yields of Glass-Maujean et al. (1987) and autoionization yields of Dehmer & Chupka (1976).
[c] Emission yields of the $v_j=0-3$ levels of the $D'\ ^1\Pi_u^-$ state are unity within experimental error.
[d] From Glass-Maujean et al. (2008b).

states have also been determined by Glass-Maujean et al. (1987) from a simultaneous experimental measurement of H_2 absorption and H Lyman-α excitation spectra, and from measurements of Fano profiles of absorption transitions. For comparison purposes, their predissociation yields are listed in parentheses in Tables 1 and 2. It can be noted that Glass-Maujean

et al. (1987) were only able to measure the lower limits of the predissociation yields of the $B''\bar{B}\ ^1\Sigma_u^+$ state. In this sense, the present study has obtained more definitive predissociation yields for the $v_j = 1$ to 4 levels of the $B''\bar{B}\ ^1\Sigma_u^+$ state. However, the two sets of values, in general, agree within error limits, though a slight difference can be noted for the $J_j = 1$ and $v_j = 1$ level of the $D'\ ^1\Pi_u^+$ state (0.88 ± 0.08 versus 0.65 ± 0.15). The predissociation yield for the $J_j = 2$ of the $5p\sigma\ ^1\Sigma_u^+(1)$ is also significantly different from that given by Glass-Maujean et al. (1987). The difference, however, arises from problems in both the adiabatic and nonadiabatic calculations. Based on the predissociation yield of Glass-Maujean et al. (1987) and the calculated $P(3)$ and $R(1)$ branch transition probabilities, the model shows that the calculated emission intensities of the $R(1)$ transition are too weak in a number of locations (e.g., 820.44 Å, 849.39 Å, 878.65 Å, 908.09 Å, and 937.57 Å) while those of the $P(3)$ transitions roughly agree with observation. Based on Hönl–London factors, the $P(3)$ transitions should be approximately 50% stronger than the $R(1)$ transitions. The nonadiabatic calculation also predicts stronger $P(3)$ branch transitions to $v_i = 0-5$ levels of the $X\ ^1\Sigma_g^+$ state. The observed intensities of the $R(1)$ transitions in many of these bands, however, are stronger than the corresponding $P(3)$ lines. It is unclear which perturbing state is responsible for the deviation in P- and R-branch relative intensities. The nearest known $np\sigma\ ^1\Sigma_u^+$ state is the $7p\sigma\ ^1\Sigma_u^+(0)$ level, which is about 249 cm^{-1} higher in energy than the $J_j = 2$ level of the $5p\sigma\ ^1\Sigma_u^+(1)$ state. The R/P branches relative intensities of the $7p\sigma\ ^1\Sigma_u^+(0)-X\ ^1\Sigma_g^+$ transitions are also significantly stronger than those implied by Hönl–London factors (see below). Simple homogeneous coupling between the $5p\sigma\ ^1\Sigma_u^+(1)$ and $7p\sigma\ ^1\Sigma_u^+(0)$ states cannot increases the R-branch intensities of both states at the expense of the P branch. The deviation of the R/P branch relative intensities requires one or more interacting $np\pi\ ^1\Pi_u$ levels such as $5p\pi\ ^1\Pi_u$ and $7p\pi\ ^1\Pi_u$ states. In any case, the intensities of the $P(3)$ and $R(1)$ lines of the $5p\sigma\ ^1\Sigma_u^+(1)-X\ ^1\Sigma_g^+$ bands can be approximately reproduced by partitioning their transition probabilities in a 2:3 ratio. The predissociation yield for $J_j = 2$ of the $5p\sigma\ ^1\Sigma_u^+(1)$ state is correspondingly lowered to ~30%. The measured predissociation yield, 0.6 ± 0.1, is obviously more accurate than the derived predissociation yield. The large difference between the two results shows that neither absolute band transition probabilities nor P/R branch relative values are calculated reliably.

In addition to the $5p\sigma\ ^1\Sigma_u^+(1)$ level, the $R(J_i-1)/P(J_i+1)$ relative intensities of the $6p\sigma\ ^1\Sigma_u^+(0)$, $6p\sigma\ ^1\Sigma_u^+(1)$, and $7p\sigma\ ^1\Sigma_u^+(0)-X\ ^1\Sigma_g^+$ transitions are also abnormally strong. The emission originating from the $5p\sigma\ ^1\Sigma_u^+(1)$, $6p\sigma\ ^1\Sigma_u^+(0)$, and $6p\sigma\ ^1\Sigma_u^+(1)$ levels can be reconciled with the essential features of observed spectrum by repartitioning the P- and R-branch transition probabilities without a change in the calculated band transition probabilities. For the $7p\sigma\ ^1\Sigma_u^+(0)$ level, however, the band transition probabilities need to increase by a factor of ~2.5, in addition to the adjustment of the P- and R-branch Hönl–London factors. Even with the adjustment in band transition probabilities, intensities of a few $7p\sigma\ ^1\Sigma_u^+(0)-X\ ^1\Sigma_g^+$ transitions are not well reproduced. In any case, while the predissociation yields obtained with these adjustments are not expected to be reliable, the inferred values for the $6p\sigma\ ^1\Sigma_u^+(0)$, $6p\sigma\ ^1\Sigma_u^+(1)$, and $7p\sigma\ ^1\Sigma_u^+(0)$ levels are consistent with those determined by Glass-Maujean et al. (1987). All other higher v_j levels of the $6p\sigma\ ^1\Sigma_u^+$ and $7p\sigma\ ^1\Sigma_u^+$ states have negligible emission yields.

5.3. Excitation and Emission Cross Sections

The calculated transition probabilities of $np\sigma\ ^1\Sigma_u^+$ and $np\pi\ ^1\Pi_u$ band systems, along with Equations (3)–(6) and collision strength coefficients of Liu et al. (1998), permit a good estimation of the cross sections of the $np\sigma\ ^1\Sigma_u^+$ and $np\pi\ ^1\Pi_u$, especially those of the $B''\bar{B}\ ^1\Sigma_u^+$ and $D'\ ^1\Pi_u$ states. The solid lines of Figures 4 and 5 show the estimated excitation cross section of the $B''\bar{B}\ ^1\Sigma_u^+ - X\ ^1\Sigma_g^+$ and $D'\ ^1\Pi_u - X\ ^1\Sigma_g^+$ band system as a function of excitation energy. The calculation of corresponding emission cross sections requires appropriate emission yields for the rovibrational levels. For the $v_j = 1-4$ levels of the $B''\bar{B}\ ^1\Sigma_u^+$ state and $v_j = 1-5$ levels of the $D'\ ^1\Pi_u$ state, the nonradiative yields listed in Tables 1 and 2 have been applied. For higher vibrational levels, the predissociation yields listed by Glass-Maujean et al. (1987) are utilized. For some rovibrational levels, lower limits of the predissociation yields were given by Glass-Maujean et al. (1987). In these cases, lower limits are used. For autoionization, the autoionization yields reported by Dehmer & Chupka (1976) have been applied. At room temperature, emission yields for rotational levels up to the $J_j = 4$ are required. Alternatively, the emission yields can be estimated from the calculated spontaneous transition probabilities and photoabsorption line width measurements of Glass-Maujean et al. (2007a, 2007b, 2007c, 2008a). While the experimental uncertainties of the width, typically ± 0.3 cm^{-1}, are somewhat too large, they can provide a rough estimate of the yields for the high v_j levels when other data are unavailable. Because emissions from these levels are generally very weak, the error in line width does not lead to significant change in the band emission cross sections, at least, for the low n Rydberg states. The emission cross sections of the $B''\bar{B}\ ^1\Sigma_u^+$ and $D'\ ^1\Pi_u$ states are indicated by dotted lines in Figures 4 and 5.

Table 3 compares excitation and emission cross sections of singlet-*ungerade* states obtained in several studies at 100 eV and 300 K. The present cross sections for the $B\ ^1\Sigma_u^+$ and $C\ ^1\Pi_u$ states differ from those reported by Liu et al. (1998) in two ways. First, excitation to H(1s)+H(2ℓ) continuum levels, neglected in Liu et al. (1998), is taken into account in the present work using oscillator strengths derived from photodissociation cross sections calculated by Glass-Maujean (1986). Second, while Liu et al. (1998) used the $B\ ^1\Sigma_u^+ - X\ ^1\Sigma_g^+$ and $C\ ^1\Pi_u - X\ ^1\Sigma_g^+$ transition probabilities of Abgrall & Roueff (1989), the present work used transition probabilities from Abgrall et al. (1993a, 1993b, 1994). The emission cross sections of the $B\ ^1\Sigma_u^+$, $C\ ^1\Pi_u$, and $B'\ ^1\Sigma_u^+$ states do not include emission originating from the H(1s)+H(2ℓ) continuum, but include continuum emission originating from the discrete levels of the $B\ ^1\Sigma_u^+$, $C\ ^1\Pi_u$, and $B'\ ^1\Sigma_u^+$ states into the $X\ ^1\Sigma_g^+$ continuum, H(1s)+H(1s). At 100 eV and 300 K, Abgrall et al. (1997) have shown that transitions to the $X\ ^1\Sigma_g^+$ continuum contributes about 27.5% and 1.5% to the $B\ ^1\Sigma_u^+$ and $C\ ^1\Pi_u$ emission cross sections, respectively. The transition probabilities of some high v_j levels of the $D\ ^1\Pi_u^-$ state have been adjusted to the experimental values of Glass-Maujean et al. (2007c). The present cross sections of the $D\ ^1\Pi_u^-$ state differs slightly from those obtained by Jonin et al. (2000). In case of the $B''\bar{B}\ ^1\Sigma_u^+$ and $D'\ ^1\Pi_u$ states, Table 3 shows that the present cross sections are significantly larger than those estimated by Jonin et al. (2000). Possible reasons for the large difference will be discussed in Section 6.

The estimated errors of the electronic-state cross sections listed in Table 3 are as follows. The errors for the $B\ ^1\Sigma_u^+$,

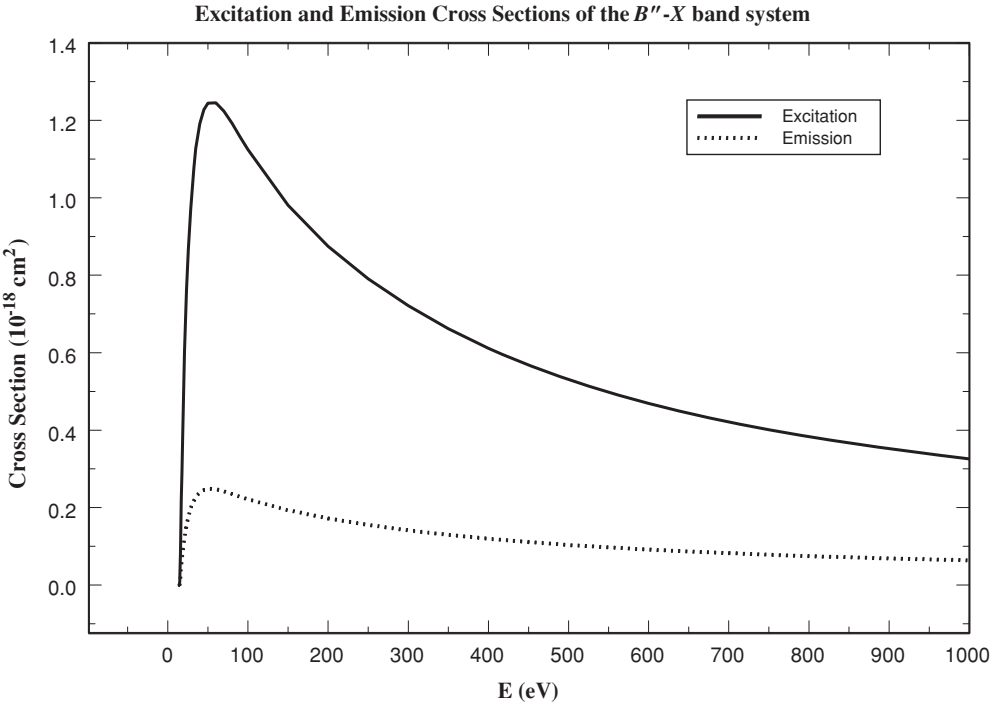

Figure 4. Excitation (solid) and emission (dotted) cross sections of the $B''\bar{B}\,^1\Sigma_u^+ - X\,^1\Sigma_g^+$ band system as a function of excitation energy at 300 K.

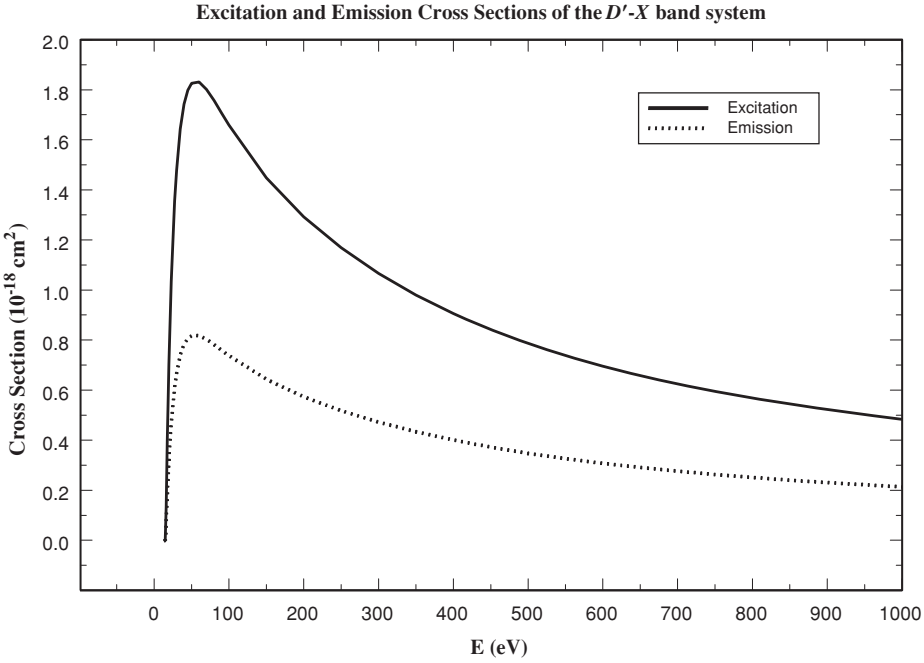

Figure 5. Excitation (solid) and emission (dotted) cross sections the $D'\,^1\Pi_u - X\,^1\Sigma_g^+$ band system as a function of excitation energy at $T = 300$ K.

$C\,^1\Pi_u$, and $D\,^1\Pi_u$ states, which primarily arise from the uncertainty in the excitation function, are no greater than 10%. For the $B'\,^1\Sigma_u^+$ and $D'\,^1\Pi_u$ states, uncertainty is less than 12%–13%. The $B''\bar{B}\,^1\Sigma_u^+(0) - X\,^1\Sigma_g^+$ emission makes a substantial contribution to the total $B''\bar{B}\,^1\Sigma_u^+$ state emission cross section. As the calculated nonadiabatic transition probabilities are unable to satisfactorily reproduce the observed relative intensities of the $R(0)$ and $P(2)$ of the $B'\,^1\Sigma_u^+(4)$ and $B''\bar{B}\,^1\Sigma_u^+(0)$ levels, there is an additional uncertainty in the $B''\bar{B}\,^1\Sigma_u^+$ state cross section, approaching to 15% for the excitation cross section and ∼18% for the emission cross section. The error limit for the $5p\sigma\,^1\Sigma_u^+$, $6p\sigma\,^1\Sigma_u^+$, and $7p\sigma\,^1\Sigma_u^+$ state emission cross sections can be as high as 25%–35% because of weak emission intensities and, more importantly, rovibronic coupling noted in Section 5.2.

6. DISCUSSION

The $v_j = 0$ level of the $B''\bar{B}\,^1\Sigma_u^+$ and $D'\,^1\Pi_u^+$ states lies below the H(1s)+H(22ℓ) dissociation limit and is, therefore, free from the predissociation of the $B'\,^1\Sigma_u^+$ continuum. Except

Table 3
Electronic-Band Cross Sections and Emission Yields of H_2 Singlet-*ungerade* States[a]

State	Present σ_{ex}	Previous σ_{ex}	Present σ_{em}	Previous σ_{em}	Present Em. Yield	Previous Em. Yield
$B\ ^1\Sigma_u^+$	264[b]	262[c]	263	262[c]	99%[b]	100%
$C\ ^1\Pi_u$	244[b]	241[c]	240[b]	241[c]	98%[b]	100%
$B'\ ^1\Sigma_u^+$	40[b]	38[d,e]	21	21[d]	53%	56%
$D\ ^1\Pi_u^+$	25	24[d]	11	11[d]	43%	46%
$D\ ^1\Pi_u^-$	21	18[d]	21	18[d]	100%	100%
$B''\bar{B}\ ^1\Sigma_u^+$	11	>4[d]	2.2	1.6[d]	20%	<40%
$D'\ ^1\Pi_u^+$	9.3	7.1[d]	1.6	1.0[d]	18%	14%
$D'\ ^1\Pi_u^-$	7.3	⩾5.3[d]	5.7	5.3[d]	78%	⩽100%
$D''\ ^1\Pi_u$	3.2	>0.6	0.9	0.6	28%	...
$5p\sigma\ ^1\Sigma_u^+$	...	...	1.1	...	...	...
$6p\sigma\ ^1\Sigma_u^+$	...	...	0.6	...	...	...
$6p\pi\ ^1\Pi_u$	...	...	0.9	...	...	...
$7p\sigma\ ^1\Sigma_u^+$	...	...	0.6	...	...	...

Notes.
[a] $E = 100$ eV and $T = 300$ K. Unit is 10^{-19} cm^2. σ_{ex} and σ_{em} denote excitation and emission cross sections, respectively. Certain numbers may not add up due to roundings. See Section 5.3 for estimated errors in cross sections.
[b] Excitation cross sections include the excitation into the H(1s)+H(2ℓ) continuum, which is estimated from the calculation of Glass-Maujean (1986). Emission cross sections exclude emission from the H(1s)+H(2ℓ) continuum levels, but include continuum emission from the excited discrete levels into the continuum levels of the $X\ ^1\Sigma_g^+$ state. Transitions to the $X\ ^1\Sigma_g^+$ continuum contribute 27.5% and 1.5%, respectively, to total emission cross sections of $B\ ^1\Sigma_u^+ - X\ ^1\Sigma_g^+$ and $C\ ^1\Pi_u - X\ ^1\Sigma_g^+$ (Abgrall et al. 1997).
[c] From Liu et al. (1998).
[d] From Jonin et al. (2000).
[e] Include excitations into the continuum levels of the $B'\ ^1\Sigma_u^+$ state.

for the $R(1)$ transitions, the adiabatic transition probabilities for the $D'\ ^1\Pi_u^+(0)$ level actually reproduces the observed relative intensities reasonably well. Very prominent discrepancies exist between the calculated and observed relative emission intensities for the $B'\ ^1\Sigma_u^+(4)$ and $B''\bar{B}\ ^1\Sigma_u^+(0)$ states. A homogeneous coupling Hamiltonian of 5.7 cm^{-1} between the $B'\ ^1\Sigma_u^+(4)$ state and $B''\bar{B}\ ^1\Sigma_u^+(0)$ state were inferred from the early absorption study of Namioka (1964b). Indeed, a simple perturbation treatment based on the Hamiltonian and adiabatic transition probabilities of the $B'\ ^1\Sigma_u^+(4)$ and $B''\bar{B}\ ^1\Sigma_u^+(0)$ states enables one to obtain good agreement between the calculated and observed spectral intensities of the $P(1)$ branch transitions. Because of the $^1\Sigma_u^+ - {}^1\Pi_u^+$ coupling, however, the simple perturbation coupling scheme fails for the transitions involving $J_j > 0$ levels.

The nonadiabatic calculation successfully reproduces the observed $P(1)$ transition intensities from the $B'\ ^1\Sigma_u^+(4)$ and $B''\bar{B}\ ^1\Sigma_u^+(0)$ levels and thus correctly accounts for the homogeneous interactions between the two vibronic levels. Except for the transitions from the $J_j = 1$ levels, the calculation reproduces the observed intensities of other J_j levels of the $B'\ ^1\Sigma_u^+(4)$ and $B''\bar{B}\ ^1\Sigma_u^+(0)$ states well within the experimental errors. For the $J_j = 1$ levels, however, discrepancies in the $R(0)$- and $P(2)$-branch absolute intensities and the $R(0)/P(2)$ relative intensities are beyond expected experimental error. Because the $J_j = 1$ levels of the $B'\ ^1\Sigma_u^+(4)$ and $B''\bar{B}\ ^1\Sigma_u^+(0)$ are strongly coupled, respectively with ∼53% and ∼47% mixture (Wolniewicz et al. 2006), the error in the coupling matrix elements is amplified. Thus, the discrepancies in $J_j = 1$ spectral intensities is most likely caused by the nonperturbative nature of nonadiatic coupling, which is inadequately approximated by the present perturbative treatment. Expanding the basis set of the calculation will probably lead to better agreement with experiment. It is also interesting to note that the nonadiabatic model overestimates the spectral intensities of the $R(1)$ and $P(3)$ branches of the $D\ ^1\Pi_u(2) - X\ ^1\Sigma_g^+(0)$ band. Since the Q-branch intensities calculated from the $D\ ^1\Pi_u^- - X\ ^1\Sigma_g^+$ transition probabilities of Abgrall et al. (1994) agree with experimental values over the entire measurement range, the small discrepancies in the $R(1)$ and $P(3)$ branches' spectral intensity also indicate the error in the nonadiabatic treatment.

The good agreement between the present and previous predissociation yields listed in Tables 1 and 2 suggests the relative accuracy of the calculated transition probabilities. As mentioned, the predissociation yield of Glass-Maujean et al. (1987) was obtained by a simultaneous measurement of molecular hydrogen absorption and atomic hydrogen Lyman-α excitation spectra. Once the absolute scale is established, the ratio of Lyman-α emission intensity to absorption intensity directly produces the predissociation yields. So, in the absence of significant spectral overlap, predissociation yields of Glass-Maujean et al. (1987) were directly obtained from measurement and, therefore, are very accurate. Predissociation yields of the present work are determined by matching the relative intensity of synthetic spectrum with that of the observed one through the adjustment of emission-branching ratio. Specifically, the accuracy of the line intensities in synthetic spectra depends on the accuracy of emission-branching ratios and the consistency of oscillator strengths (i.e., transition probabilities) among different rovibronic excitations. The good agreement in the two sets of predissociation yield, therefore, shows the good consistency among the calculated transition probabilities of the $B\ ^1\Sigma_u^+$, $C\ ^1\Pi_u$, $B'\ ^1\Sigma_u^+$, $D\ ^1\Pi_u$, $B''\bar{B}\ ^1\Sigma_u^+$, and $D'\ ^1\Pi_u - X\ ^1\Sigma_g^+$ band systems.

The excitation and emission cross sections of $B''\bar{B}\ ^1\Sigma_u^+$ and $D'\ ^1\Pi_u$ states at 100 eV excitation energy have been estimated by Jonin et al. (2000) based on modeling and extrapolating a number of experimental emission lines. For the $B''\bar{B}\ ^1\Sigma_u^+$ state at 100 eV excitation energy, Jonin et al. (2000) obtained 0.4×10^{-18} cm^2 as the lower limit of the excitation cross section, 0.16×10^{-18} cm^2 for the emission cross section, and 40% as the upper limit of the emission yield. Those numbers can be

compared with the present values of 1.1×10^{-18} cm^2 for the excitation cross section, 0.29×10^{-18} cm^2 for the emission cross section, and 21% for the band emission yield (see Table 3). For the $D'\,^1\Pi_u$ state at the same excitation energy, Jonin et al. (2000) derived 1.2×10^{-18} cm^2, 0.63×10^{-18} cm^2, and 52%, respectively, for the excitation and emission cross sections, and emission yield. These numbers can be compared with 1.7×10^{-18} cm^2 and 0.70×10^{-18} cm^2, and 42%, respectively, obtained in the present work. The probable causes for this significant difference are that the relative instrumental sensitivity between 800 Å and 850 Å were overestimated by Jonin et al. (2000) and that significant portions of the $D'\,^1\Pi_u - X\,^1\Sigma_g^+$ transition takes place in this spectral region. Furthermore, the extrapolation of the inaccurate instrumental sensitivity into the 760 to 800 Å region by Jonin et al. (2000) also contributed to the errors in the $D'\,^1\Pi_u$ state.

The calculated transition probabilities of the $np\sigma\,^1\Sigma_u^+$ and $np\pi\,^1\Pi_u - X\,^1\Sigma_g^+$ ($n = 4-8$) band systems, adiabatic or nonadiabatic, represent an important step toward accurate modeling of the electron-impact induced emission spectrum of H_2 in the wavelength region below 900 Å. Liu et al. (1995), Abgrall et al. (1997), and Jonin et al. (2000) have shown that models utilizing the calculated transition probabilities for the $B\,^1\Sigma_u^+ - X\,^1\Sigma_g^+$, $C\,^1\Pi_u - X\,^1\Sigma_g^+$, $B'\,^1\Sigma_u^+ - X\,^1\Sigma_g^+$, and $D\,^1\Pi_u - X\,^1\Sigma_g^+$ band systems by Abgrall et al. (1993a, 1993b, 1993c, 1994, 2000) can accurately reproduce experimental H_2 spectral intensities between the 1040 Å and 1660 Å wavelength region. Measurement and analysis by Jonin et al. (2000) have also demonstrated that emissions from $B''\bar{B}\,^1\Sigma_u^+$, $D'\,^1\Pi_u$, and higher $np\sigma\,^1\Sigma_u^+$ and $np\pi\,^1\Pi_u$ states are not negligible in certain spectral regions below 1040 Å. Between 900 Å and 1040 Å, emissions from the $B\,^1\Sigma_u^+ - X\,^1\Sigma_g^+$, $C\,^1\Pi_u - X\,^1\Sigma_g^+$, $B'\,^1\Sigma_u^+ - X\,^1\Sigma_g^+$, and $D\,^1\Pi_u - X\,^1\Sigma_g^+$ band systems contribute over 95% of the total H_2 emission intensity, with the $B''\bar{B}\,^1\Sigma_u^+ - X\,^1\Sigma_g^+$ and $D'\,^1\Pi_u - X\,^1\Sigma_g^+$ band systems contributing another ~3%. Jonin et al. (2000) have noted that the observed relative intensities for some (i.e., "strong") emissions from the $v_j = 0$ and 1 levels of the $B'\,^1\Sigma_u^+$ state are significantly stronger than their calculated counterparts. The discrepancy was attributed to the cascade excitation of the low-v_j levels of the $B'\,^1\Sigma_u^+$ state (Liu et al. 2002). The present work shows that the available transition probabilities can accurately account for over 99% of the molecular hydrogen spectral intensity in the 900 Å to 1040 Å wavelength region. Emissions from higher-Rydberg ($n \geqslant 5$) states become significant on the blue side of 900 Å, with the lower $B'\,^1\Sigma_u^+$, $C\,^1\Pi_u$, $B'\,^1\Sigma_u^+$, $D\,^1\Pi_u$, $B''\bar{B}\,^1\Sigma_u^+$, and $D'\,^1\Pi_u$ states contributing about 90%–92% to the total observed spectral intensities between 790 Å and 900 Å. In a few small wavelength regions, emissions from the 5pσ, 6pσ, 7pσ, 5pπ, 6π, and 7π are the dominant spectral features. The differences between the model and observation for a few transitions of the $B'\,^1\Sigma_u^+(4)$, $D\,^1\Pi_u^+(2)$, $B''\bar{B}\,^1\Sigma_u^+(0)$, $6p\sigma\,^1\Sigma_u^+(0)$, $6p\sigma\,^1\Sigma_u^+(1)$, and $7p\sigma\,^1\Sigma_u^+(0)$ levels are beyond experimental error, which is 8%–12% for moderately strong transitions. The overall emission intensity from these levels, however, is less than 2% of the total emission intensity between 790 Å and 900 Å. The current model is thus capable of reproducing ~98% of e+H_2 emission intensity at room temperature and 100 eV excitation energy within experimental error.

The present work makes it possible to improve the accuracy of calibration for the *Cassini Ultraviolet Imaging Spectrograph* (*UVIS*) instrument. Before this work, the relative sensitivity of the *UVIS* instrument in the spectral direction of the EUV region was established with the electron-impact induced emission spectrum of H_2 (Shemansky & Liu 2000), based on the model and experimental spectra of Jonin et al. (2000). As the spectra of Jonin et al. (2000) is accurate only for the wavelength region above 900 Å, it was difficult to obtain an accurate calibration for the *UVIS* instrument in the shorter wavelength region. Indeed, the large point-spread function of *UVIS* actually limited the accurate calibration to the $\lambda > 920$ Å region (Shemansky & Liu 2000). The present work has not only extended the accurate calibration into the 800−920 Å region but has also improved the accuracy above 920 Å. The present results, along with those obtained in Abgrall et al. (1997) and Jonin et al. (2000), make it possible to obtain accurate relative sensitivity curves of laboratory spectrometers and *Cassini UVIS* instrument over the range 800 Å to 1630 Å.

Electron-impact excitation of H_2 in the atmospheres of outer planets usually takes place at temperatures higher than 300 K (e.g., 500−1200 K), over a wide range of electron excitation energies. Accurately modeling the emission intensity in the EUV region obviously requires emission yields for the higher J_j levels. Nevertheless, assuming that the predissociation and autoionization yields for the high J_j levels of the $B'\,^1\Sigma_u^+$ and $D'\,^1\Pi_u$ states are similar to those of the low J_j levels, the calculated transition probabilities of the $B\,^1\Sigma_u^+$, $C\,^1\Pi_u$, $B'\,^1\Sigma_u^+$, $D\,^1\Pi_u$, $B''\bar{B}\,^1\Sigma_u^+$, $D'\,^1\Pi_u$, and higher $np\sigma\,^1\Sigma_u^+$ and $np\pi\,^1\Pi_u - X\,^1\Sigma_g^+$ band systems, along with those involved in the cascade excitation via the singlet-*gerade* states (Liu et al. 2002), provide basic physical parameters for an accurate interpretation of spacecraft observations of the electron-impact induced emission spectrum of H_2 over the entire VUV region.

In summary, adiabatic transition probabilities of the $np\sigma\,^1\Sigma_u^+$ and $np\pi\,^1\Pi_u - X\,^1\Sigma_g^+$ ($n = 4-8$), and nonadiabatic transition probabilities of the $B'\,^1\Sigma_u^+$, $B''\bar{B}\,^1\Sigma_u^+$, and $D\,^1\Pi_u^+ - X\,^1\Sigma_g^+$ band systems have been obtained. The high-resolution electron impact-induced emission spectrum of H_2 obtained by Jonin et al. (2000) and Liu et al. (2000) has been re-examined with presently and previously calculated transition probabilities. Adiabatic transition probabilities are found to be consistent with experimental observation when localized rovibronic coupling of the $np\sigma\,^1\Sigma_u^+$ and $np\pi\,^1\Pi_u$ states is insignificant. When localized coupling is significant, nonadiabatic calculations are partially successful in removing the discrepancies between model and observation. Emission yields obtained by comparison of calculated and experimental intensities also agree with the predissociation yield reported by Glass-Maujean et al. (1987) and autoionization yield by Dehmer & Chupka (1976). Refined excitation and emission cross sections for the $B''\bar{B}\,^1\Sigma_u^+$, $D'\,^1\Pi_u$, and several higher Rydberg states have been obtained.

The work at the Space Environment Technologies (SET) has been supported by the *Cassini UVIS* contract with the University of Colorado, and NASA-NNG06GH76G issued to SET through the Planetary Atmospheres Program. We thank Charles Malone for valuable suggestions.

REFERENCES

Abgrall, H., & Roueff, E. 1989, A&AS, 79, 313
Abgrall, H., & Roueff, E. 2006, A&A, 445, 361
Abgrall, H., Roueff, E., & Drira, I. 2000, A&AS, 141, 297
Abgrall, H., Roueff, E., Launay, F., & Roncin, J. Y. 1994, Can. J. Phys., 72, 856
Abgrall, H., Roueff, E., Launay, F., Roncin, J. Y., & Subtil, J. L. 1993a, A&AS, 101, 273

Abgrall, H., Roueff, E., Launay, F., Roncin, J. Y., & Subtil, J. L. 1993b, A&AS, 101, 323
Abgrall, H., Roueff, E., Launay, F., Roncin, J. Y., & Subtil, J. L. 1993c, J. Mol. Spectrosc., 157, 512
Abgrall, H., Roueff, E., Liu, X., & Shemansky, D. E. 1997, ApJ, 481, 557
Abgrall, H., Roueff, E., Liu, X., Shemansky, D. E., & James, G. K. 1999, J. Phys. B: At. Mol. Opt. Phys., 32, 3813
Ajello, J. M., Shemansky, D. E., Kwok, T. L., & Yung, Y. L. 1984, Phys. Rev. A, 29, 636
Ajello, J. M., Srivastava, S. K., & Yung, Y. L. 1982, Phys. Rev. A, 25, 2485
Ajello, J. M., et al. 1988, Appl. Opt., 27, 890
Ajello, J. M., et al. 1998, J. Geophys. Res., 103, 20125
Allison, A. C., & Dalgarno, A. 1970, At. Data Nucl. Data Tables, 1, 289
Clarke, J. T., Jaffel, L. B., Vidal-Madjar, A., Gladstone, G. R., Waite, J. H., Jr., Prangé, R., Gérard, J.-C., & Ajello, J. M. 1994, ApJ, 430, L73
Dabrowski, I. 1984, Can. J. Phys., 62, 1639
Dehmer, J. L., Dehmer, P. M., Pratt, S. T., Tomkins, F. S., & O'Halloran, M. A. C. 1989, J. Chem. Phys., 90, 6243
Dehmer, J. L., Dehmer, P. M., West, J. B., Hayes, M. A., Siggel, M. R. F., & Parr, A. C. 1992, J. Chem. Phys., 97, 7911
Dehmer, P. M., & Chupka, W. A. 1976, J. Chem. Phys., 65, 2243
Dehmer, P. M., & Chupka, W. A. 1995, J. Phys. Chem., 99, 1686
De Lange, A., Hogervorst, W., & Ubachs, W. 2001, Phys. Rev. Lett., 86, 2988
Ekey, R. C., Jr., Marks, A., & McCormack, E. F. 2006, Phys. Rev. A, 73, 023412
Feldman, P. D., McGrath, M. A., Moos, H. W., Durrance, S. T., Strobel, D. F., & Davidsen, A. F. 1993, ApJ, 406, 279
Glass-Maujean, M. 1979, Chem. Phys. Lett., 68, 320
Glass-Maujean, M. 1986, Phys. Rev. A., 33, 342
Glass-Maujean, M., & Beswick, J. A. 1989, J. Chem. Soc., Faraday Trans. 2, 85, 983
Glass-Maujean, M., Breton, J., & Guyon, P. M. 1978, Phys. Rev. Lett., 40, 181
Glass-Maujean, M., Breton, J., & Guyon, P. M. 1979, Chem. Phys. Lett., 63, 591
Glass-Maujean, M., Breton, J., & Guyon, P. M. 1984, Chem. Phys. Lett., 112, 25
Glass-Maujean, M., Breton, J., & Guyon, P. M. 1985a, J. Chem. Phys., 83, 1468
Glass-Maujean, M., Breton, J., & Guyon, P. M. 1987, Z. Phys. D., 5, 189
Glass-Maujean, M., Breton, J., Thieblemont, B., & Ito, K. 1985b, Phys. Rev. A, 32, 947
Glass-Maujean, M., Breton, J., Thieblemont, B., & Ito, K. 1985c, in Photophysics and Photochemistry above 6eV, ed. F. Lahmani (Amsterdam: Elsevier Science), 405
Glass-Maujean, M., Klumpp, S., Werner, L., Ehresmann, A., & Schmoranzer, H. 2007a, J. Phys. B, 40, F19
Glass-Maujean, M., Klumpp, S., Werner, L., Ehresmann, A., & Schmoranzer, H. 2007b, J. Chem. Phys., 126, 144303
Glass-Maujean, M., Klumpp, S., Werner, L., Ehresmann, A., & Schmoranzer, H. 2007c, Mol. Phys., 105, 1535
Glass-Maujean, M., Klumpp, S., Werner, L., Ehresmann, A., & Schmoranzer, H. 2008a, J. Mol. Spectrosc., 249, 51
Glass-Maujean, M., Klumpp, S., Werner, L., Ehresmann, A., & Schmoranzer, H. 2008b, J. Chem. Phys., 128, 94312
Greetham, G. M., Hollenstein, U., Seiler, R., Ubachs, W., & Merkt, F. 2003, Phys. Chem. Chem. Phys., 5, 2528
Gustin, J., et al. 2004, Icarus, 171, 336
Guyon, P. M., Breton, J., & Glass-Maujean, M. 1979, Chem. Phys. Lett., 68, 314
Hansson, A., & Watson, J. K. G. 2005, J. Mol. Spectrosc., 233, 169
Herzberg, G., & Howe, L. L. 1959, Can. J. Phys., 37, 636
Herzberg, G., & Jungen, Ch. 1972, J. Mol. Spectrosc., 41, 425
Hilborn, R. C. 1982, Am. J. Phys., 50, 982
Hinnen, P. C., Hogervorst, W., Stolte, S., & Ubachs, W. 1994a, Appl. Phys. B, 59, 307
Hinnen, P. C., Hogervorst, W., Stolte, S., & Ubachs, W. 1994b, Can. J. Phys., 72, 1032
Hinnen, P. C., & Ubachs, W. 1995b, Chem. Phys. Lett., 240, 351
Hinnen, P. C., & Ubachs, W. 1996, Chem. Phys. Lett., 254, 32
Hinnen, P. C., Werners, S. E., Stolte, S., Hogervorst, W., & Ubachs, W. 1995a, Phys. Rev. A, 52, 4425
Hogervorst, W., Eikema, K. S. E., Reinhold, E., & Ubachs, W. 1998, Nucl. Phys. A, 631, 353
Hollenstein, U., Reinhold, E., de Lange, C. A., & Ubachs, W. 2006, J. Phys. B., 39, L195
Jonin, C., Liu, X., Ajello, J. M., James, G. K., & Abgrall, H. 2000, ApJS, 129, 247
Julienne, P. J. 1971, Chem. Phys. Lett., 8, 27
Jungen, Ch., & Atabek, O. 1977, J. Chem. Phys., 66, 5584
Kim, Y. H., Caldwell, J. J., & Fox, J. L. 1995, ApJ, 447, 906
Koelemeij, J. C. J., de Lange, A., & Ubachs, W. 2003, Chem. Phys., 287, 349
Kolos, W., & Wolniewicz, L. 1968, J. Chem. Phys., 48, 3672
Larzillière, M., Launay, F., & Roncin, J.-Y. 1985, Can. J. Phys., 63, 1416
Liu, X., Ahmed, S. M., Multari, R. A., James, G. K., & Ajello, J. M. 1995, ApJS, 101, 375
Liu, X., Shemansky, D. E., Abgrall, H., Roueff, E., Dziczek, D., Hansen, D. L., & Ajello, J. M. 2002, ApJS, 138, 229
Liu, X., Shemansky, D. E., Ahmed, S. M., James, G. K., & Ajello, J. M. 1998, J. Geophys. Res., 103, 26739
Liu, X., Shemansky, D. E., Ajello, J. M., Hansen, D. L., Jonin, C., & James, G. K. 2000, ApJS, 129, 267
Morrissey, P. F., Feldman, P. D., Clarke, J. T., Wolven, B. C., Strobel, D. F., Durrance, S. T., & Trauger, J. T. 1997, ApJ, 576, 918
Namioka, T. 1964a, J. Chem. Phys., 40, 3154
Namioka, T. 1964b, J. Chem. Phys., 41, 2141
O'Halloran, M. A., Dehmer, P. M., Pratt, S. T., Dehmer, J. L., & Tomkins, F. S. 1989, J. Chem. Phys., 90, 930
O'Halloran, M. A., Dehmer, P. M., Tomkins, F. S., Pratt, S. T., & Dehmer, J. L. 1988, J. Chem. Phys., 89, 75
Pratt, S. T., Dehmer, J. L., Dehmer, P. M., & Chupka, W. A. 1992, J. Chem. Phys., 97, 3038
Pratt, S. T., Dehmer, J. L., Dehmer, P. M., & Chupka, W. A. 1994, J. Chem. Phys., 101, 882
Pratt, S. T., McCormack, E. F., Dehmer, J. L., Dehmer, P. M., & Chupka, W. A. 1990, J. Chem. Phys., 92, 1831
Reinhold, E., Hogervorst, W., & Ubachs, W. 1996, J. Mol. Spectrosc., 180, 156
Reinhold, E., Hogervorst, W., & Ubachs, W. 1997, Phys. Rev. Lett., 78, 2543
Roncin, J.-Y., & Launay, F. 1994, Atlas of the Vacuum Ultraviolet Emission Spectrum of Molecular Hydrogen (J. Phys. Chem. Ref. Data, Monograph No. 4, Washington, DC: Amer. Chem. Soc.)
Roncin, J.-Y., Launay, F., & Larzilliere, M. 1984, Can. J. Phys., 62, 1686
Ross, S., & Jungen, Ch.1987, Phys. Rev. Lett., 59, 1297
Ross, S., & Jungen, Ch.1994a, Phys. Rev. A, 49, 4353
Ross, S., & Jungen, Ch.1994b, Phys. Rev. A, 49, 4364
Ross, S., & Jungen, Ch.1994c, Phys. Rev. A, 49, 4618
Ross, S., & Jungen, Ch.1997, Phys. Rev. A, 55, 2503
Shemansky, D. E., & Liu, X. 2000, Cassini UVIS Tech. Rep., USC101300-02
Staszewska, G., & Wolniewicz, L. 2002, J. Mol. Spectrosc., 212, 208
Stephens, J. A., & Greene, C. H. 1994, J. Chem. Phys., 100, 7135
Takezawa, S. 1970, J. Chem. Phys., 52, 2575
Trafton, L. M., Gérard, J. C., Munhoven, G., & Waite, J. H., Jr. 1994, ApJ, 421, 816
Ubachs, W., & Reinhold, E. 2004, Phys. Rev. Lett., 92, 101302
Vigué, J., Beswick, J. A., & Broyer, M. 1983, J. Phys. (Paris), 44, 1225
Wolniewicz, L. 1993, J. Chem. Phys., 99, 1851
Wolniewicz, L., Orlikowski, T., & Staszewska, G. 2006, J. Mol. Spectrosc., 238, 118
Wolniewicz, L., & Staszewska, G. 2003a, J. Mol. Spectrosc., 220, 45
Wolniewicz, L., & Staszewska, G. 2003b, J. Mol. Spectrosc., 217, 181
Wolven, B. C., & Feldman, P. D. 1998, Geophys. Res. Lett., 25, 1537